

# **Studies in synchronization phenomena in Physical and Biological Systems**

*A dissertation submitted in partial fulfilment of the degree of*  
**Master of Technology in Computational Techniques**

By  
**Nishant Malik**

JUNE, 2008



**SCHOOL OF PHYSICS  
UNIVERSITY OF HYDERABAD  
Hyderabad-500046,India**

## DECLARATION

I hereby declare that the dissertation entitled “**Studies in Synchronization phenomena in Physical and Biological systems**” submitted to University of Hyderabad in partial fulfilment of the requirement for the award of the degree of **Master of Technology in Computational Techniques** is an original work done by me during my course of study under the guidance of **Dr. Janaki Balakrishnan**, Reader, School of Physics, University of Hyderabad, Hyderabad-500046, India and has not been submitted for the award of any degree or diploma in any other university.

**June-2008**  
**Hyderabad**

**NISHANT MALIK**  
M.Tech(Computational Techniques)  
Reg No:-06PHQT06



## CERTIFICATE

This is to certify that the dissertation entitled “**Studies in synchronization phenomena in Physical and Biological systems**” being submitted by **Mr. Nishant Malik** in partial fulfilment of the requirement for the award of the degree of **Master of Technology in Computational Techniques**, to the School of Physics, University of Hyderabad, Hyderabad, is an original research work carried out by him under my supervision and has not formed the basis for the award of any other degree, diploma or title by this institution or any other University.

**Dr. Janaki Balakrishnan**

Reader, School of Physics,  
University of Hyderabad,  
Hyderabad-500046, India

**Dean,**

School Of Physics,  
University of Hyderabad  
Hyderabad-500046, India

**Place: Hyderabad**

**Date:**

To

*my parents and teacher*

## ACKNOWLEDGEMENTS

My utmost gratitude goes to my supervisor Dr. Janaki Balakrishnan whose help, stimulating suggestions and unflinching encouragement and immense patience has made this work possible. I am indebted to her for host of other things too : for exposing me to different facets of scientific research in nonlinear dynamics, helping me in learning different aspects of this fascinating subject, above all and the most needed, for giving me immense freedom to explore issues on my own. She has inspired and enriched my growth as a student.

I am deeply indebted to Dr. B. Ashok for numerous valuable discussions which have been truly educative for me. I am also deeply grateful for his constant and unhesitating support to me during the past one year.

I would like to acknowledge many other teachers of mine who have exposed me to different aspects of numerics and computation during my academics. Most notable among them is Prof. Vijay Verma at the University of Delhi who taught me a two semester course on computational physics during my M.Sc(Physics). Prof K.P.N. Murthy for offering that marvelous course on Monte-Carlo simulations in the II<sup>nd</sup> semester of M.Tech. Dr. Ashoka Vudayagiri for being very supportive during a course on Advanced Scientific Computing Laboratory in I<sup>st</sup> semester.

I thank many of the faculty members in the School of Physics and Department of Computer Science who taught me different courses in first year of my M.Tech. I would also like to thank Dr. Venkatesh Shenoi for helping me in learning GNUPLOT and LATEX, his friendly guidance has always been of great help to me both in academic and personal life. A major part of this work was carried out at CMSD (Center for Modelling Simulation and Design), I want to thank CDAC staff members at CMSD, Ratan and Srinivas for providing me atmosphere congenial for work.

My deepest gratitude goes to my family for their unflagging love and support throughout my life; this project would have been simply impossible without them. I am indebted to my father, Dr. G.R Malik, for his care and love. He has spared no effort to provide me the best possible environment for me to grow up. I cannot ask for more from my mother, Mrs. Usha Malik, as

she is simply perfect. I have no suitable word that can fully describe her everlasting love to me. I remember her constant support when I encountered difficulties and I remember, most of all, her delicious dishes. I also thank my younger brother Prashant for being very supportive and caring for all these years.

I also wish to thank my friends Tarak, Madhumita and other classmates of M.Tech(C.T) and my roommate Venkat who has suffered a lot due to my odd hour work schedule for their help and encouragement. I express my sincere thanks to my friends Supriya, Satish and Sita Rama Raju for their inspirational support.

The financial support of the University of Hyderabad is gratefully acknowledged.

*Nishant Malik*

## PUBLICATIONS

1. **Noise-induced synchronous activity in coupled theta neurons**

– Nishant Malik, J. Balakrishnan and B. Ashok

(Proceedings of the National Conference on Nonlinear Systems and Dynamics (NCNSD — 2008) held at Physical Research Laboratory , Ahmedabad, India during Jan 03-05 ,2008).

2. **Noise-induced firing and synchronization in a system of coupled theta neurons**

– Nishant Malik , J.Balakrishnan and B.Ashok (2008) (submitted).

3. **Synchronization in coupled Class I neurons: the role of noise**

– Nishant Malik , J.Balakrishnan and B.Ashok (2008) (submitted)

## ABSTRACT

A study of noise induced synchronization phenomena in neural firing activity of coupled Class-I spiking neurons is presented . The model studied is that of a system of generic oscillators supporting saddle node bifurcation on an invariant circle called theta neuron coupled together. Coupling realized through a gating variable and a set of parameters describing its coupling strength and synapse type. The gating variables are governed by feedback equations which depend upon the output of the neurons they couple. We study both bidirectional and unidirectional coupling configurations with different combinations of synapses.

Using various techniques of nonlinear dynamics such as nonlinear time series analysis, methods of bifurcation theory and calculation of lyapunov exponents, we study the rich dynamical structure of the emergent collective behaviour of the coupled neuronal system. We observe that introducing common white noise to this system induces synchronous activity in it. We have made use of Hilbert transforms and statistical interpretation of phase differences in the presence of noise to show phase synchronization in some of the cases where complete synchronization was found to be elusive. We find that noise can increase the rate of firing. We calculate Lyapunov exponents for the system in the presence of noise which gives us insights into the combinations of synaptic strengths and couplings required for the neurons to undergo complete synchronization.

In a simulation of a neuronal ensemble containing 200 theta neurons with 150 excitatory and 50 inhibitory synapses and with all to all coupling, we have shown synchronous firing of all the neurons on introduction of weak white noise .

**Keywords:** synchronization, saddle node bifurcation, theta neuron, lyapunov exponent, noise induced firing, noise induced synchronization

# Contents

<b>1</b>	<b>Introduction</b>	<b>3</b>
<b>2</b>	<b>Synchronization</b>	<b>7</b>
2.1	Introduction . . . . .	7
2.2	Types of synchronization . . . . .	8
2.2.1	Mutual Synchronization . . . . .	9
2.2.2	Complete Synchronization . . . . .	9
2.2.3	Phase and Frequency locking : weaker forms of synchrony . . . . .	12
2.2.4	Generalized Synchronization . . . . .	13
2.3	Noise induced synchronization . . . . .	14
2.4	Examples of synchronization . . . . .	15
2.5	Role of Synchronization in neuronal systems . . . . .	16
<b>3</b>	<b>Neuron Models</b>	<b>18</b>
3.1	Introduction . . . . .	18
3.2	The Neuron . . . . .	19
3.3	Hodgkin-Huxley model . . . . .	22
3.4	Morris-Lecar model . . . . .	24
3.5	Classification of neural excitability and corresponding generic bifurcations .	25
3.5.1	Hodgkin Classification of neural excitability . . . . .	25
3.5.2	Review of some relevent codimension 1 bifurcations . . . . .	26
3.6	Theta Neuron model . . . . .	27
3.7	Coupled Theta Neurons . . . . .	30
3.8	Dynamics of a pair of coupled Theta Neurons . . . . .	33

<b>4</b>	<b>Noise induced Synchronization and firing in coupled theta neuron</b>	<b>38</b>
4.1	Introduction . . . . .	38
4.2	Neuronal Noise . . . . .	39
4.3	Noise term in coupled theta neuron . . . . .	40
4.4	Noise induced firing in coupled theta neuron . . . . .	41
4.5	Noise induced complete synchronization in coupled theta neurons . . . . .	43
4.6	Instantaneous phase-frequency plots . . . . .	49
4.7	Noise induced phase synchronization in IE coupling . . . . .	51
4.8	A simulation of an ensemble of 200 neurons . . . . .	52
4.9	Further studies and Conclusion . . . . .	54
4.9.1	Further Studies . . . . .	54
4.10	Conclusion . . . . .	56
<b>A</b>	<b>Lyapunov Exponents</b>	<b>57</b>
<b>B</b>	<b>Hilbert Transform</b>	<b>61</b>
<b>C</b>	<b>Stochastic RK-4</b>	<b>63</b>

# Chapter 1

## Introduction

The scientist does not study nature because it is useful; he studies it because he delights in it, and he delights in it because it is beautiful. If nature were not beautiful, it would not be worth knowing, and if nature were not worth knowing, life would not be worth living.

**J.Henri Poincaré**

---

Synchronization is one of those phenomena in nature which transcends the boundaries of different disciplines and which manifests in nearly every branch of the natural sciences, in engineering and also in social life. Synchronization is encountered in various systems: from electrical power systems to fireflies emitting sequence of light pulses, from the chirping of crickets to ensembles of neurons, from pendulum clocks to the Belousov-Zhabotinsky reaction. Scientists hailing from physics, genetics, psychology, chemistry, entomology, engineering, computer science and mathematics are constantly uncovering new examples of it[1]. Even coupled chaotic systems can undergo a transition to synchronization. This in fact finds applications in communication. Recent evidence shows that common noise can also induce synchronization in nonlinear oscillators including in the chaotic ones. This is quite counterintuitive as noise is always equated with disorder.

Synchronous phenomena have attracted the interest of scientists over the centuries, Historically, it was mainly investigated in man made devices like pendulum clocks, electronic devices, electric power systems, etc. Discovered by Christiaan Huygens in 17th century while he was lying ill in bed, he observed that two pendulum clocks hanging from the

same support beam swung in perfect anti-phase. He also very much correctly inferred that this synchrony between the clocks is due to the motion imparted to the beam by the pendulum clock; this motion is of course imperceptible. The basis of synchronization is interaction between two individual units — these individual units could be pendula, neurons or fireflies. This interaction can often lead to synchronous activity emerging between these units. That is what exactly Huygens also inferred.

In broad terms we can define synchronization as an adjustment of rhythms of oscillating objects due to their weak interactions[2]. The relevance of Synchronous phenomena and their manifestation across such a broad array of disciplines is due to the presence of vast numbers of these oscillating objects around us. It seems that synchronization is one of the fundamental features of such systems. Real oscillators occurring in nature are nonlinear. This fact has, in the the last few decades influenced the way we study synchronization. The analytical and numerical methods and tools of nonlinear dynamics are now used to analyze synchronization phenomena. These methods and tools make it possible to predict the types and strength of coupling which could lead to synchronization, and to study the stability of synchronized state in the presence of perturbations. In the study presented, we have made use of several of such techniques such as Hilbert transform, methods of bifurcation theory and calculation of lyapunov exponents.

Synchronization has many forms and the emergence of a functional relationship between variables governing the dynamics of the system is a consequence of a type of synchronization called generalised synchronization (GS). Complete Synchronization(CS) is a special case of this [2]. In CS the time evolution of the coupled systems is identical. CS is also the rarest form of synchrony observed because it requires the coupled systems to be identical in every respect and real systems are rarely identical. In non-identical systems phase synchronization (PS) and frequency synchronization (FS) are commonly encountered forms of synchrony. In these kinds of synchronization the phase or the frequency of coupled systems get locked. In chapter one we discuss types of synchronization in detail.

Biological systems abound with examples of rhythmic processes like beating of the heart, the opening and closing of ion channels in cell membranes, blood cell levels, the process of respiration, the daily cycle of waking and sleeping and many more processes vital for living organisms. Some diseases occur due to abnormalities in the biological rhythms. Mathematically these rhythms can be modelled through nonlinear equations

and since analytical solutions can be often difficult to obtain in such equations, we need to resort to numerical simulations to understand these rhythms[3]. Because of the important role played by rhythms in nature, scientific interest in synchronization phenomena in physical and biological systems has grown manifold. In this dissertation we present a study of a biological system — a pair of coupled neurons. It is thought that synchronous firing of neurons plays a central role in the way the brain performs some cognitive tasks such as visual perception, feature extraction and recognition, etc. A key element in neuronal information processing is phase synchronization of neurons. On the other hand synchronous phenomena can also have negative effects for instance increased synchrony can also lead to pathological types of activity such as epilepsy. In neurosciences there is an ongoing endeavor to understand the precise mechanism and conditions under which neurons synchronize.

An important feature associated with biological systems is the presence of random fluctuations in their rhythms or what we call “noise”. The origin of these fluctuations can be traced even upto the cellular level in biological systems. For example the opening and closing of ion channels in cell membranes is a stochastic process. Noise is inherent in biological processes and it becomes very important to study the biological processes and systems by taking this noise into account. So apart from the already present nonlinearities in biological rhythms, now we have models with stochastic variables too. This makes study of a biological system a formidable task even with modern day computers. Noise can induce many interesting phenomena. For example when noise of optimal intensity is presented to a nonlinear system it can lead to amplification of a weak input signal or an enhanced response by the system — an effect known in the literature as “stochastic resonance” (in externally driven systems) or “coherence resonance” (in autonomous systems)[4]. Noise can also induce synchronization — this is a phenomenon which is still not a well understood.

Neurons can be modelled as non-linear oscillators. In our work we have investigated the effects of noise on the coupled dynamics of a special class of neurons[5],[6],[7]. We have studied noise induced synchronized activity and firing in coupled theta neurons having excitatory-excitatory and inhibitory-excitatory interactions, coupled both unidirectionally as well as bidirectionally. A theta neuron is described by a normal form equation for a saddle-node bifurcation on invariant circle, bifurcation generic for neurons with Class-I

excitability, the classification of neural excitability dating back to Hodgkin. The coupling between these neurons is realized through synaptic conductances whose time evolution is modelled with ordinary differential equations. The ODE for each synaptic gating variable depends on the output of the presynaptic neuron. It is known that Class-I oscillators are difficult to synchronize[8],[9]. We aimed to study noise – induced Synchronization in such a system. We show and study complete synchronization in a system of coupled theta neurons induced by common white noise. We also try to decipher the dynamics of this system by using the techniques of stability analysis, Lyapunov exponent and Hilbert transform. We also present some work regarding the weaker form of synchrony in nonidentical coupled theta neurons meaning when we have inhibitory-excitatory (I-E); we are able to show that noise does induce order in such cases also. Calculation of the Lyapunov exponent for E-E as well as I-E system have not been done previously in the literature. We present those here for the first time.

A realistic small scale model of brain should consist of ensembles of neurons, each having sufficiently large number of spiking neurons with different bifurcation dynamics and coupled according to some physiological basis. Under what conditions does synchronous activity emerge in such an ensemble? Computational effort and resources to model even a small such ensemble with real physiological conditions and parameters put in would be no mean task. However one can attempt to capture key features of the real system using appropriate simplified generic models. We have in our work included a simulation of an ensemble of 200 generic class-I theta neurons bidirectionally coupled in an all to all manner with both excitatory and inhibitory couplings.

# Chapter 2

## Synchronization

Some twenty years ago I saw, or thought I saw, a synchronal or simultaneous flashing of fireflies. I could hardly believe my eyes, for such a thing to occur among insects is certainly contrary to all natural laws.[10]

**Philip Laurent**

---

### 2.1 Introduction

Synchronization can be defined as the process of adjustment of rhythms of two weakly interacting oscillators. In a system it can manifest as mere adjustment of phase or frequency without affecting the amplitude of the system; in the more fascinating situation, the frequency, phase and amplitude of the oscillators all get synchronized. This form of synchronization is called the complete synchronization (CS). This chapter is a review of some basic literature and known results on synchronization, beginning with a little historical note.

#### Historical Note

The first reference to the phenomena of synchronization in scientific literature is found in the works of Christiaan Huygens, the Dutch mathematician and physicist. In some of the letters written to his father during February 1665, he talks about synchronous motion between two pendulum clocks interacting through a beam connecting the clocks. He describes this phenomena as “*sympathy of two clocks*”. Also an observation of synchro-

nization in acoustic systems exists in the famous treatise *The Theory of Sound* compiled in the middle of the 19th century by J. William Strut (Lord Rayleigh).

Early theoretical studies on synchronization were made by E.V. Appleton and B. van der Pol. During 1920's they worked on triode generators and showed that the frequency of the generator can be entrained or synchronized by weak external signal of slightly different frequency. This work had lot of practical importance in radio communication systems.

Among early observations of synchronization of biological rhythms, mention may be made of the first recorded observation of synchronous flashing in a large population of fireflies by Englebert Kempter<sup>1</sup> around 1680 during his voyage to Thailand. In 1729 the French astronomer and mathematician Jean-Jacques Dortous de Mairan recorded his observations of biological rhythms in haricot bean plant. According to his observations the leaves of the plant changed their orientations as day turned to night an example of synchronization of biological cycles with earth's daily cycle[2].

## 2.2 Types of synchronization

Before proceeding further we need to discuss a little more about different forms of synchrony observed. These forms are discussed in detail in the next few sections of the chapter. In our work we are most interested in complete synchronization. If we have two weakly coupled oscillators and after little transient due to the presence of this weak coupling they undergo a transition to a state where their time evolution becomes the same in terms of phase, frequency and amplitude, such a transition is termed as complete synchronization. The weak coupling between them could be deterministic or non-deterministic i.e introduction of weak common noise can lead to a transition to CS[11]. Let the time evolution of two systems be described by the variables  $y_1(t)$  and  $y_2(t)$  respectively. If due to a weak interaction between these two systems a relationship of the sort  $y_1(t) = \phi(y_2(t))$  emerges where  $\phi$  is invertible, the two systems are said to be under generalized synchronization (GS). In case of CS  $\phi$  is identity. It is also possible that only either phase or frequency of the two oscillators gets locked and amplitude of these oscillators remain uncorrelated, such kinds of synchronization are termed as phase locking or frequency locking respectively.

---

<sup>1</sup>Dutch physician

### 2.2.1 Mutual Synchronization

In this chapter and subsequent chapters we have focussed our study on synchronization between two coupled oscillators. This type of synchronization is referred to as mutual synchronization in the literature. We have discussed mutual synchronization both in deterministic systems, i.e when there are no random fluctuations, and also in the non-deterministic case, i.e, in the presence of random fluctuations or noise. We have in our work not considered cases in which synchronous activity is observed between an external drive and the oscillator i.e when there is only a driving by a source but no feedback to influence the source.

### 2.2.2 Complete Synchronization

Complete Synchronization can be classified further into local and global synchronization. Local synchronization is stable – small perturbations cannot desynchronize the system. In global synchronization, the system approaches synchronous dynamics asymptotically. So whatever might be the initial condition, the system will ultimately synchronize. In the next part of this section we look at mathematical conditions required to be satisfied for a system to undergo a transition to these simplest forms of CS. First we look at conditions for coupled linear equations and then for coupled non-linear equations. Later we will discuss CS in chaotic systems.

#### Case I. Coupled linear system

Consider a linear system

$$\dot{\mathbf{X}} = \mathbf{A}\mathbf{X} \quad (2.1)$$

where  $\mathbf{A}$  is an  $n \times n$  matrix. Now we introduce a coupling  $c$  in the following way in the above system

$$\dot{\mathbf{X}}_1 = \mathbf{A}\mathbf{X}_1 + c(\mathbf{X}_2 - \mathbf{X}_1) \quad (2.2)$$

$$\dot{\mathbf{X}}_2 = \mathbf{A}\mathbf{X}_2 + c(\mathbf{X}_1 - \mathbf{X}_2) \quad (2.3)$$

writing the the above equation in matrix form as

$$\begin{pmatrix} \dot{\mathbf{X}}_1 \\ \dot{\mathbf{X}}_2 \end{pmatrix} = \begin{pmatrix} \mathbf{A} - c & c \\ c & \mathbf{A} - c \end{pmatrix} \begin{pmatrix} \mathbf{X}_1 \\ \mathbf{X}_2 \end{pmatrix} \quad (2.4)$$

Defining the difference  $\mathbf{Y} = \mathbf{X}_1 - \mathbf{X}_2$  then from above equations we get

$$\dot{\mathbf{Y}} = (\mathbf{A} - 2c\mathbf{I})\mathbf{Y} \quad (2.5)$$

Now if the eigen values of  $\mathbf{A}$  are  $\lambda_1, \lambda_2, \dots, \lambda_n$  the eigen values of  $\mathbf{A} - 2c\mathbf{I}$  will be  $\lambda_1 - 2c, \lambda_2 - 2c, \dots, \lambda_n - 2c$ . The condition for having asymptotically stable equilibrium point at origin for Eq(2.5) is  $Re(\lambda_i) < 2c$ . It means that when this particular condition is satisfied above system undergoes global synchronization i.e

$$\lim_{t \rightarrow \infty} \mathbf{Y}(t) = \lim_{t \rightarrow \infty} |\mathbf{X}_1(t) - \mathbf{X}_2(t)| = 0 \quad (2.6)$$

Otherwise if origin is only stable equilibrium point then system undergoes local synchronization .

## Case II. Coupled non-linear system

Let a general autonomous system be described by :

$$\dot{\mathbf{X}} = f(\mathbf{X}) \quad (2.7)$$

Then consider the pair of systems coupled through a parameter  $c$  as follows:

$$\dot{\mathbf{X}}_1 = f(\mathbf{X}_1) + c(\mathbf{X}_2 - \mathbf{X}_1) \quad (2.8)$$

$$\dot{\mathbf{X}}_2 = f(\mathbf{X}_2) + c(\mathbf{X}_1 - \mathbf{X}_2) \quad (2.9)$$

On linearizing Eq.(2.7) we will get

$$\begin{pmatrix} \dot{\mathbf{X}}_1 \\ \dot{\mathbf{X}}_2 \end{pmatrix} = \begin{pmatrix} \mathbf{A}(t) - c\mathbf{I} & c\mathbf{I} \\ c\mathbf{I} & \mathbf{A}(t) - c\mathbf{I} \end{pmatrix} \begin{pmatrix} \mathbf{X}_1 \\ \mathbf{X}_2 \end{pmatrix} \quad (2.10)$$

$$\dot{\mathbf{X}} = \mathbf{A}(t)\mathbf{X} \quad (2.11)$$

where the matrix  $\mathbf{A}(t) = D_{\mathbf{X}}(f(\mathbf{X}_1(t)))$  is evaluated along the synchronized trajectory  $\mathbf{X}_1(t) = \mathbf{X}_2(t)$ .

For the above case there exists a synchronization theorem[12] which we state it below without proof.

**Theorem 2.1** :- If  $\lambda_1$  is the largest Lyapunov exponent of system described by Eq.(2.7) & by the coupling is two way as in the coupled equations Eq.(2.8) & Eq.(2.9) and  $c > \lambda_1/2$ , then the coupled system satisfies local synchronization. That is, the synchronized state  $\mathbf{Y}(t) = \mathbf{X}_1(t) - \mathbf{X}_2(t) = 0$  is a stable equilibrium.

## Complete Synchronization in coupled chaotic system

System exhibiting chaotic behaviour show sensitive dependence on initial conditions. Hence two independently evolving chaotic systems, though identical do not synchronise. Pecora and Corroll.[13] showed however that by introducing an appropriate coupling between them, it is possible to synchronise even chaotic systems. Their important work finds applications in secure communications of digital and analog signals in chaotic cryptography etc. This type of synchronization is termed as master-slave synchronization. They used the Lorenz system as an example to show CS in chaotic systems.

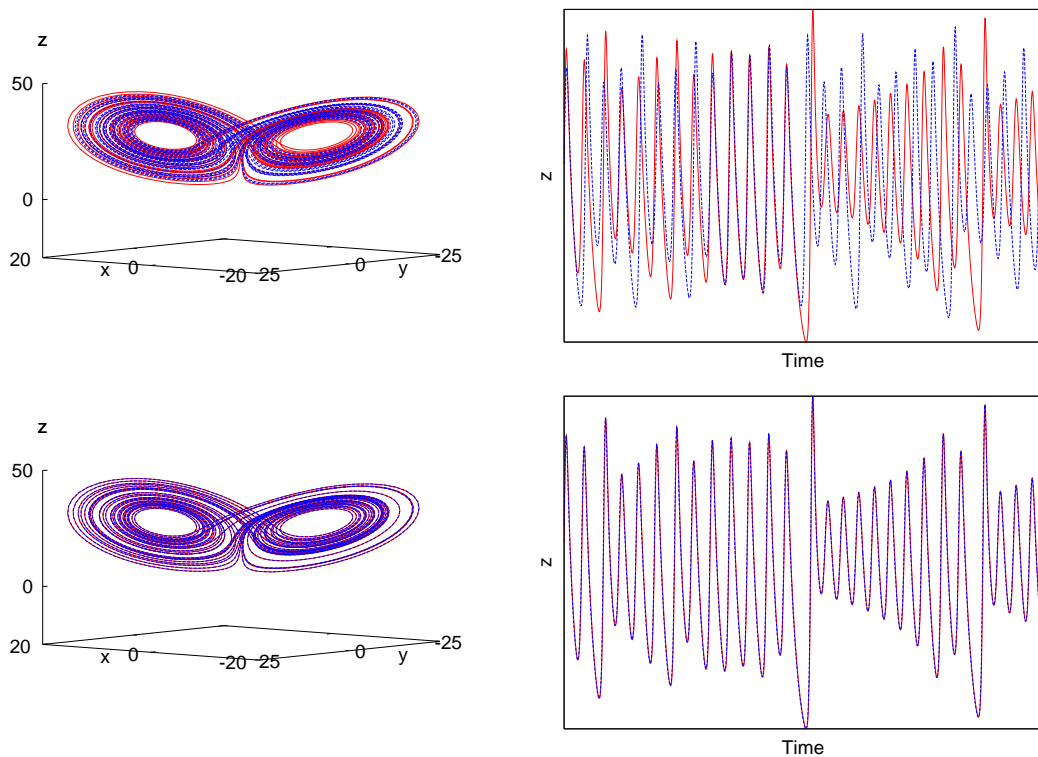


Figure 2.1: Output of two Lorenz's systems at different initial conditions (Left: Lorenz attractor ,Right: Time series for z-variable),in upper panel two systems are uncoupled and in lower panel they are coupled as master(red) and slave(blue)

The master-slave coupling was achieved in the following way. The first Lorenz system described by the variables  $(x_1, y_1, z_1)$  may be taken to be the sender or the master and the second Lorenz system  $(x_2, y_2, z_2)$  as the receiver or slave. The equations representing

the master system are

$$\begin{aligned}
\dot{x}_1 &= -\sigma x_1 + \sigma y_1 \\
\dot{y}_1 &= -x_1 z_1 + r x_1 - y_1 \\
\dot{z}_1 &= x_1 y_1 - b z_1
\end{aligned} \tag{2.12}$$

and the slave is given by

$$\begin{aligned}
\dot{x}_2 &= -\sigma x_1 + \sigma y_2 \\
\dot{y}_2 &= -x_1 z_2 + r x_1 - y_2 \\
\dot{z}_2 &= x_1 y_2 - b z_2
\end{aligned} \tag{2.13}$$

Eq(2.13) represent the slave system since it contains a signal  $x_1$  from its master, or the sender,Eq(2.14). An implementation of the Pecora – Carroll method is shown in fig 2.1 in which we have taken the initial condition for the master system  $x_1 = -15.0, y_1 = 12.0, z_1 = 11.5$  and those for the slave to be  $x_2 = -15.05, y_2 = 12.1, z_2 = 11.0$ . The values of the other parameters were as follows  $\sigma = 10.0, r = 28.0, b = 8.0/3.0$ . We observe that the two chaotic systems having different initial conditions and evolving independently now have the same time evolution. This result has practical application in the control of chaos and communication systems.

It is also possible to achieve similar sort of synchronization using the coupling discussed in Section(2.2.2).The coupling term will be proportional to the differences  $(x_1 - x_2, y_1 - y_2, z_1 - z_2)$  and at the transition to CS these couplings will become zero so that each system will become free of the other’s influence at this stage. Hence one obtains two identical chaotic systems (same values of parameters) starting at different initial conditions but having same time evolution after some transients governed by the synchronization theorem 2.1[14].

### 2.2.3 Phase and Frequency locking : weaker forms of synchrony

#### Phase Locking

Synchronous activity can also emerge in the phases and frequencies of the system without affecting the amplitude. If the phase difference of two oscillators becomes a constant then that situation is termed as phase-locking. Let  $\phi_1$  and  $\phi_2$  denote the phases of the two

oscillators and let  $\Delta\phi$  denote their difference. Then one can have  $\Delta\phi = 0$  corresponding to in phase synchronization, and  $\Delta\phi = \pi$  corresponding to antiphase or out of phase synchronization Fig(2.2.3). The coupling has two totally distinct effects on phases – either it brings them together or it takes them apart. One could also have higher order phase-locking in an  $n : m$  ratio defined by  $|n\phi_1 - m\phi_2| < \text{constant}$ .

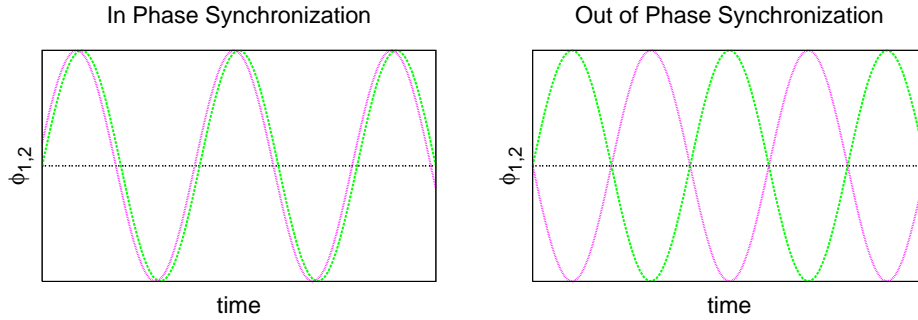


Figure 2.2: Possible forms of phase synchronization. Left: in-phase synchronization . Right: Out of phase synchronization

## Frequency Locking

Let  $\omega_1$  and  $\omega_2$  denote the frequencies of the oscillators when they are uncoupled. On coupling, the frequencies of these interacting oscillators change to  $\Omega_1$  and  $\Omega_2$ . If the coupling is sufficiently strong then a state can be reached at which  $\Omega_1 = \Omega_2 = \Omega$ , and one then says that oscillators are frequency locked  $\Omega$  typically being  $\omega_1 < \Omega < \omega_2$ . The condition for higher order frequency locking i.e in a ratio  $m : n$  is  $m\Omega_1 = n\Omega_2$ , generally this occurs when in the uncoupled system one has  $m\omega_1 \simeq n\omega_2$

### 2.2.4 Generalized Synchronization

When we have nonidentical systems coupled together, strictly speaking it is difficult to observe CS. It might be possible that for sufficiently strong couplings a functional relation emerges between the variables of the two interacting systems. For instance if  $\mathbf{x}_1$  and  $\mathbf{x}_2$  represents the dynamical variables of two non-identical interacting systems, a functional relationship of the form  $\mathbf{x}_1 = \mathbf{F}(\mathbf{x}_2)$  could emerge between the two systems. This implies that if  $\mathbf{F}$  is known then the state of the second system can be determined. This regime is called generalized synchronization (GS). It is usually observed for the cases where we

have unidirectional coupling or what is also known as master–slave coupling. CS is just a case of generalized synchronization where  $\mathbf{F}$  becomes an identity.

## 2.3 Noise induced synchronization

Till now we have only considered the deterministic case. Interestingly, common noise can also induce synchronization in a system of coupled oscillators including chaotic ones. Oscillators in nature are always subject to some natural fluctuations and these fluctuations can be modelled by some random process, or noise. The interpretation of phase in the presence of noise requires a statistical approach. In the presence of noise phase becomes a stochastic variable and both phase  $\phi_{1,2}(t)$  and phase difference  $\Delta\phi(t) = \phi_1(t) - \phi_2(t)$  perform motion similar to Brownian motion. Their evolution can therefore be regarded as performing random walk in a potential and this observed phenomenon is called *phase diffusion*. Synchronization induced by noise is usually interrupted by abrupt changes in the phase difference called *phase slips*[4]. If the noise is weak and bounded then it never causes phase slips whereas in the case of strong bounded noise or unbounded noise (e.g. Gaussian), phase slips occur and hence phase locking and frequency locking cannot be defined in a manner similar to that defined above for the deterministic case. In the presence of noise we look at the distribution of  $\Delta\phi(t)$  on a circle  $[0, 2\pi]$  or  $[-\pi, \pi]$ . A peak in this distribution is indicative of a preferred phase difference which we can consider as a condition for phase locking in the presence of noise[2].

### Noise induced synchronization in chaotic systems

Introduction of common noise in a system of two identical chaotic systems coupled together can induce complete synchronization in them. A condition necessary for this to happen is that the largest Lyapunov exponent (Chaotic systems have positive non-zero largest Lyapunov exponent) become negative at the transition to the synchronized state[11]. In reality, systems are typically not identical and CS is difficult to observe in nonidentical systems. Further it has been shown in numerical studies that in coupled non-identical chaotic systems zero Lyapunov exponent becomes negative undergoing noise induced phase synchronization[11]. Where the phase synchronization’s interpretation was taken in statistical sense as described in the previous section.

## 2.4 Examples of synchronization

Synchronization is observed in various physical, chemical and biological systems. The purpose of this section is to demonstrate the phenomena of synchronization in different real systems. We have only discussed very few examples from the huge number of available ones, but these examples will be ample proof of the fact that synchronization is a very widely occurring phenomena in nature.

***Coupled Pendulum clocks:-*** Historically, one of the first observations of the phenomenon of synchronization was recorded by Christiaan Huygens around 1665. He was also the inventor of pendulum clock. He recorded the motions of two pendulum clocks suspended by hooks from a wooden beam. He noted that the motions of each pendulum in opposite swings were in exact agreement with each other. These clocks were able to establish this agreement in their motion even if they were perturbed a little. From this Huygens inferred that synchrony in motion was due to the motion of the beam which was not quite perceptible. His observation was that of an anti-phase mutual synchronization of the clocks due to the coupling via the beam.

***Triode Generators:-*** Another important historical example of observation of synchronization was made by E.V Appleton in 1922 in his experiment with two coupled triode generators. Each generator had an amplifier(triode vacuum tube), an  $LC$ -circuit acting as an oscillator and a feedback implemented by connecting another inductance. The coupling was realised by placing the coils of the two circuits nearby so that their magnetic fields overlapped. The frequency of one of the circuit was varied by putting a variable capacitor. Appleton observed that as the frequency of the circuit was varied, the second circuit was able to reset its frequency and synchronize with the first one.

***Belousov-Zhabotinsky Reaction:-*** Periodic optical forcing of light sensitive Belousov-Zhabotinsky reaction can transform a rotating spiral wave pattern to a labyrinthine pattern. The two domains in labyrinthine pattern oscillate (changing intensity) with a natural frequency of  $f_o = 0.028Hz$ . Varying the frequency of the periodic optical forcing produces a sequences of frequency locked regimes[15].

***Acoustic synchrony in snowy tree Cricket:-*** The Snowy tree cricket(*Oecanthus fultoni*) is a white or pale green coloured insect found in the United States, is sometimes called the thermometer cricket because it has been observed that its chirps are easily countable and their rate correlates well with the temperature of the place. Snowy tree

crickets have this ability to synchronize their chirps by responding to the preceding chirps of their neighbours. If a neighbour's chirp precedes its own, a cricket shortens its chirp in the following interval. If it follows his own, he lengthens his chirp interval and sometimes the following chirp. To establish this T.J. Walker[16] performed an experiment in which he played a prerecorded chirp continuously to male crickets kept inside a separate glass container. He found also that these insects can achieve synchrony very fast, i.e. within two cycles.

***Synchrony in fireflies:-*** Since hundreds of years travellers to Southeast Asia were perplexed on seeing mass synchrony in flashing congregations of fireflies. They popularised it by writing about it on their return. It is known that male fireflies emit rhythmic light pulses to attract females (they have light emitting cells in their abdomen). It has been observed that they can synchronize their flashes with their neighbours. The modern study of synchrony in fireflies dates from 1968, when John and Elisabeth Buck used cine photography and photometry to demonstrate that a certain number of Southeast Asian firefly species flash in rhythmic synchrony [17]. As each firefly in a congregation can be treated as individual oscillator, so studies were carried out on how single fireflies respond to a stimulant. It was found that firefly adjusts its flashing cycle with its neighbour by resetting its phase and changing the frequency of its flash. It is one of the best examples of emergence of collective synchronization in living organism.[1]

***Synchrony in predator-prey cycles*** Synchrony can also be observed in spatially extended ecological systems. A popular example is the prey-predator cycle. The most studied among the different predator-prey cycle is the one concerning the Canadian hare-lynx cycle. A very strange fact about them is that the abundance of the species in different regions of Canada get phase synchronized. Their amplitudes remain uncorrelated and vary chaotically. The migration of these animals between different regions act as kind of coupling or interaction. The abundances oscillate regularly and periodically in phase and this interaction induces a synchronization in phase.[18]

## **2.5 Role of Synchronization in neuronal systems**

Synchronization is thought to be the central mechanism for neuronal information processing and also for communication between different areas of the brain. It plays key role in

the visual perception . Visual features in an image are perceptually grouped when populations of neurons in separate parts of the cortex synchronize their activities. Motor control depends on integration and co-ordination of information in sensorimotor cortex and there is evidences that this becomes possible due to the synchronization of oscillatory activity in the sensorimotor cortex. Synchronization of neurons in sensorimotor cortex helps in the integration and coordination of information underlying motor control. Even abnormal forms of synchronization in neurons can cause some disorders like epilepsy. It has been found to be responsible for generation of pathological tremors. Many vital rhythms like respiration in the body are synchronized and these rhythms are produced by synaptically coupled pacemaker neurons in the lower brainstem. It is possible to measure synchronized firing of neurons by EEG (electroencephalography). A usual observation from the spectral analysis of EEG is that neurons can oscillate in various frequency bands. Another important observation is that in neuronal ensembles, neurons fire in synchrony when different stimuli (like visual,odorous etc) are applied to them [19].

# Chapter 3

## Neuron Models

The sciences do not try to explain, they hardly even try to interpret, they mainly make models. By a model is meant a mathematical construct which, with the addition of certain verbal interpretations, describes observed phenomena. The justification of such a mathematical construct is solely and precisely that it is expected to work.

**Johann Von Neumann**

---

### 3.1 Introduction

The brain is one of the most intricate objects in nature and its building blocks are the neurons. Without understanding the dynamics of a single neuron it will be impossible to understand fully how the brain does all the computations. There are many mathematical models of a single neuron constructed to capture some of the features of its dynamics like bursting, excitability, threshold behavior etc. In this chapter we briefly outline the biological aspects of a neuron and then we briefly review three mathematical neuron models, viz. Hodgkin–Huxley, Morris–Lecar and Theta Neuron model. We have added a short note on the classification of neuron models based on bifurcations.

The simplest and minimal model to mimic the dynamics of the brain could be a pair of neurons connected through some dynamical couplings. In this chapter we also present some of the results we have obtained in our study about the dynamics of a pair of theta neurons coupled through dynamically evolving variables based on biologically plausible synaptic conductances.

## 3.2 The Neuron

Neurons are the basic computational units of the nervous system and constitute a major part of the brain, the other constituent elemental units of the brain being the neuroglia and Schwann cells. The brain consists of around  $10^{11}$  neurons. Each neuron on an average is connected to 10,000 other neurons. There is even a diversity in the types of neurons on the basis of different shapes, sizes, forms and functions. Their ability to transmit electric signals rapidly over large distances distinguishes them from any other cells in the body. These electric signals are referred to as action potentials or nerve impulses or spikes. Fig(3.1) illustrates the structure of a typical neuron. A typical neuron has four

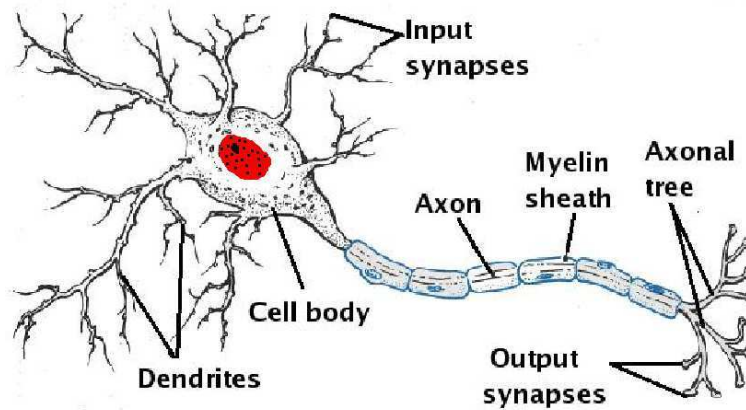


Figure 3.1: Structure of typical neuron

important morphological features— dendrites, cell body, axon and pre-synaptic terminals. The dendrites receive the inputs from other cells— the branches of the dendrites allow a neuron to receive inputs from many other neurons through synaptic connections. The cell body is the metabolic center of the neuron. The inputs received through dendrites are processed and integrated in the cell body and sent through the axon hillock in the form of an action potential through the axon which carries neuronal output from one cell to other. They can be very long and can traverse the whole body. Axons are usually covered with an envelope of myelin sheath which is made of phosphorated fats. The axon also sends out branches which allow the output to be directed to many locations on muscle cells or other neurons. The terminal end of an axon divides into fine branches that have specialized swellings called the presynaptic terminals; these are the transmitting elements of neurons. The junction between the axon and the dendrite of a target neuron across which they communicate is called a synapse. In later part of this section we will discuss

synapses further [9][20][21][22].

## Ion Gates

A neuron is enclosed by a membrane which separates the intracellular fluid from the extracellular fluid. The cell membrane is a thin bilayer of lipids and it is impermeable to most of the charged molecules. Most of the time a concentration difference exists between the inside and the outside of the neuron, with negative ions being in excess inside the neuron. This happens because of the presence of pore-forming proteins in the membrane which act as ion gates. There are two types of these ion gates of which the ones that create and maintain this concentration gradient are called the ion pumps and the others are ion channels which give the ability of selective permeability to the membrane. These ion channels allow ions to move in and out of the cell and thus control the flow of ions by opening and closing in response to voltage changes and to both internal and external signals. The membrane conductance depends on the density of ion channels present on the membrane and the conductance of individual channels depend on many different factors including the membrane potential. The most predominant ions involved in the ionic mechanisms of a neuron are sodium  $Na^+$ , potassium  $K^+$ , calcium  $Ca^{2+}$  and chloride  $Cl^-$ . In the resting state of a neuron,  $Na^+$  concentration is higher outside the neuron whereas  $K^+$  has higher concentration inside[22].

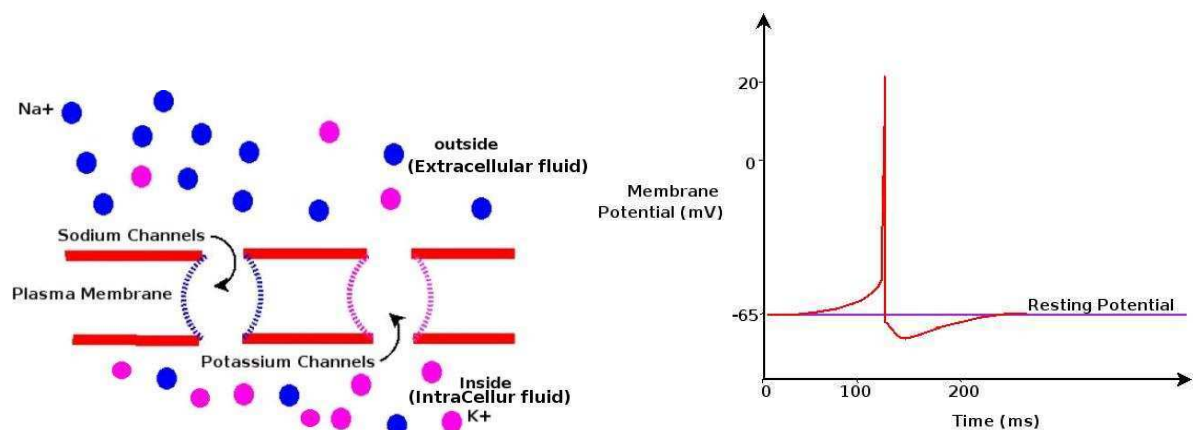


Figure 3.2: Left :Ion Channels embedded in the cell membrane. Right: An action potential showing the time scale and voltage involved in its generation (recorded from a cultured rat neocortical pyramidal cell) [22]

## Action Potential

The unequal concentration of ions between the intracellular and extracellular fluids leads to generation of electric potential called the resting potential. Empirically its value has been found to be around  $-65mV$ . The process of generation of an action potential involves very rapid depolarization of the membrane. When an external current is injected into the neuron it leads to opening of sodium channels. As a result there is heavy influx of  $Na^+$  into the membrane, which in turn sets in a positive feedback process making the potential more positive and it shoots to  $20mV$ . At this point the  $K^+$  channels open and the potential returns to  $-75mV$  and then again slowly relaxes to resting potential by releasing  $Cl^-$  ions. This whole process gets over within  $1ms$ . An action potential proceeds along the axon by successive excitation of segments of the membrane in the way described above. The speed of propagation of the action potential varies between 1 and  $100m/s$ . The importance of action potential is due to their ability to cover large distances at a rapid rate[22].

## Synapses

Neurons are connected to each other through synapses. Among the two types of synapses i.e. chemical and electrical, the chemical synapses are more common in the vertebrate brain. In chemical synapses the terminal point of the axon has a large bulb like shape which consists of vesicles which have neurotransmitters in them. There is no direct contact between the presynaptic and postsynaptic neurons but a small gap having a width of about  $20nm$  exists between them called the synaptic cleft. The working of chemical synapses involves a complicated set of steps. When a nerve impulse arrives at an axon terminal it leads to an inward flow of calcium ions. These calcium ions induce a complex process called exocytosis in the vesicles which causes release of neurotransmitters into the synaptic cleft. These neurotransmitters have the ability to influence the conductivity of postsynaptic membrane. At these stages two entirely different effects can be observed. If the postsynaptic membrane depolarizes then we say that an excitatory postsynaptic potential has been induced and the corresponding synapse is termed as excitatory. Otherwise if hyperpolarization of the postsynaptic membrane occurs then such a synapse is called inhibitory and the effect induced is an inhibitory postsynaptic potential. In electrical synapses electrical impulses are exchanged directly between the neurons through

openings in the cell membrane and hence these are also known as gap junctions. Unlike chemical synapses they are bidirectional and also the time required for current flow is lesser[21],[23].

### 3.3 Hodgkin-Huxley model

In the early 1950's Alan Lloyd Hodgkin and Andrew Huxley carried out a series of electrophysiological experiments on the giant axon of the Atlantic squid (*Loligo pealei*), using voltage clamps. Based on these experiments they modelled the ionic events which occur during the generation of the action potential by means of a set of differential equations[24]. Hodgkin and Huxley were awarded Noble prize in Physiology or Medicine for this work in 1963. In the Hodgkin–Huxley model the ionic current has three components classified by their carrier ions, viz., sodium ions  $I_{Na}$ , potassium ions  $I_K$  and a small leakage current  $I_l$  due to chloride ions. The cell membrane has selective permeability and it acts as a separator between the extracellular liquid and interior of the cell and its action is analogous to a capacitor. A Nernst Potential develops due to the concentration gradient in ions between the inside and the outside of the cell. This potential is represented by the battery in Fig(3.3) which is the circuit representation of the Hodgkin–Huxley model.

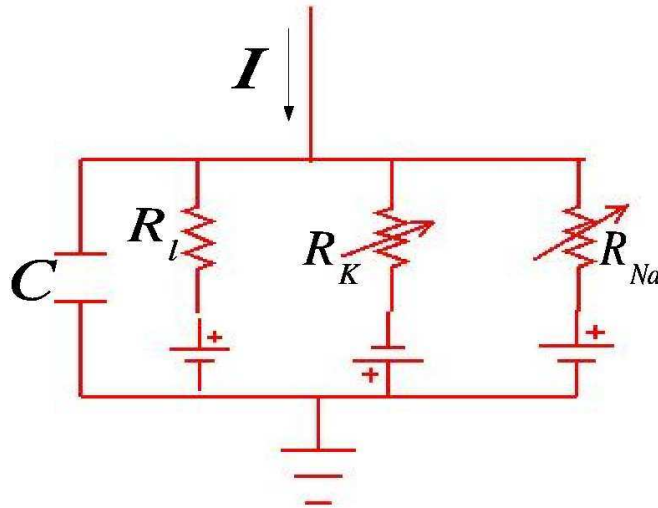


Figure 3.3: Circuit representation of Hodgkin-Huxley model

The total current  $I$  in the circuit is given as :

$$I = I_C + I_{ionic} \quad (3.1)$$

Where  $I_{ionic}$  is the total ionic current &  $I_C$  is the capacitor current. If  $V$  is the displacement of the membrane potential from its resting value and  $C$  represent membrane capacitance per unit area then we will have  $I_C = C \frac{dV}{dt}$  with the total ionic current  $I_{ionic} = I_{Na} + I_K + I_l$ . The conductance of the ionic current has relative dependence on the number of open ion channels. To take this dependence into account Hodgkin and Huxley introduced gating variables  $m, h$  for  $Na^+$  ions and  $n$  for  $K^+$  ions. The individual ionic currents are given as follows

$$\begin{aligned} I_{Na} &= g_{Na} m^3 h (V - E_{Na}) \\ I_K &= g_K n^4 (V - E_K) \\ I_l &= g_l (V - E_l) \end{aligned} \quad (3.2)$$

where  $g_{Na}, g_K$  are the maximum possible conductances of  $Na^+$  and  $K^+$  ion channels respectively.  $g_l = 1/R$  is conductance of the leakage current  $E_{Na}, E_K$  and  $E_l$  stands for reversal potential. Eq(3.1) can be written as

$$I = C \frac{dV}{dt} + g_{Na} m^3 h (V - E_{Na}) + g_K n^4 (V - E_K) + g_l (V - E_l) \quad (3.3)$$

Where  $g_{Na}, g_K, g_l, E_{Na}, E_K$  and  $E_l$  are all empirical parameters. The gating variables  $m, h$  and  $n$  variables are dynamical and they are governed by first order rate equations with voltage dependent parameters[21].

$$\begin{aligned} \dot{m} &= \alpha_m(V)(1 - m) - \beta_m(V)m \\ \dot{n} &= \alpha_n(V)(1 - n) - \beta_n(V)n \\ \dot{h} &= \alpha_h(V)(1 - h) - \beta_h(V)h \end{aligned} \quad (3.4)$$

$\alpha$  and  $\beta$  are obtained by fitting experimental data. At temperature  $6.3^\circ C$  these voltage dependent parameters are given as

$$\begin{aligned} \alpha_m &= \frac{0.1(25 - V)}{\exp[(25 - V)/10] - 1}, & \alpha_n &= \frac{0.01(10 - V)}{\exp[(10 - V)/10] - 1} \\ \alpha_h &= 0.07 \exp(-V/20), & \beta_m &= 4 \exp(-V/18) \\ \beta_n &= 0.125 \exp(-V/80), & \beta_h &= \frac{1}{\exp[(30 - V)/10] + 1} \end{aligned} \quad (3.5)$$

The formulation represented by Eq(3.3), Eq(3.4) and Eq(3.5) forms the Hodgkin-Huxley model of a neuron[25].

### 3.4 Morris-Lecar model

This model was developed by C.Morris and H.Lecar in 1981 based on electrophysiology of the muscle fiber of the barnacle (*Balanus nubilus*)[26]. When subject to constant current input the muscles fibre produce oscillatory voltage waveforms as their response. The original form of this model has three variables but here we present a simplified version of it which has only two variables. The muscle fiber of a giant barnacle has only two types of channels  $K^+$  and  $Ca^{2+}$ . The Morris -Lecar model has two types of ionic currents, an outward going potassium current and an inward going calcium current. Assuming the  $Ca^{2+}$  current to have a faster time scale than that of  $K^+$ , we have the following set of ODE's

$$\begin{aligned}\frac{dV}{dt} &= I - g_l(V - V_l) - g_K w(V - V_K) - g_{Ca} m_\infty(V)(V - V_{Ca}) \\ \frac{dw}{dt} &= \lambda(V)(w_\infty(V) - w)\end{aligned}\tag{3.6}$$

with

$$\begin{aligned}m_\infty(V) &= 0.5(1 + \tanh(\frac{V - V_1}{V_2})) \\ w_\infty(V) &= 0.5(1 + \tanh(\frac{V - V_3}{V_4})) \\ \lambda(V) &= \phi \cosh(\frac{V - V_3}{2V_4})\end{aligned}\tag{3.7}$$

where,  $g_K$  and  $g_{Ca}$  are potassium and calcium conductances respectively and  $g_l$  is the leakage conductance.  $V_K$ ,  $V_{Ca}$  and  $V_l$  are the corresponding reversal potentials .  $w$  represents the fraction of  $K^+$  channels which are open. The  $Ca^{2+}$  channels are assumed to get activated instantaneously.  $w_\infty$  and  $m_\infty$  are gating variables, and  $V_1, V_2, V_3, V_4$  and  $\phi$  are constants.

The values of the constants are as follows :-  $g_K = 2.0$ ,  $g_{Ca} = 1.33$ ,  $g_l = 0.5$ ,  $V_K = -0.7$ ,  $V_{Ca} = 1$ ,  $V_l = -0.5$ ,  $V_1 = -0.01$ ,  $V_2 = 0.15$ ,  $V_3 = 0.1$ ,  $V_4 = 0.145$ ,  $\phi = 1/3$ .

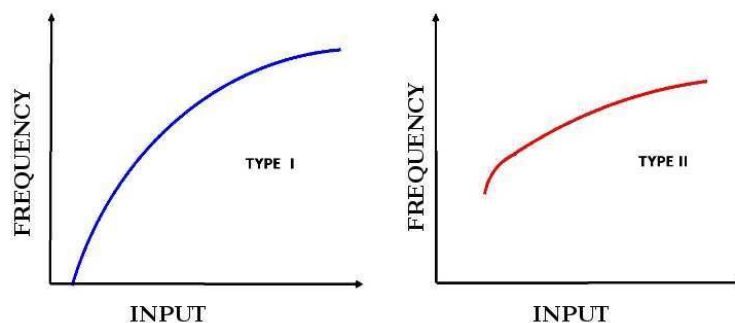


Figure 3.4: Input response curves for type I and type II excitability

## 3.5 Classification of neural excitability and corresponding generic bifurcations

Before proceeding further, to the next model we will give brief outline of the classification of neurons based on their dynamics – their excitability patterns and associated bifurcations. We will also use some of the concepts introduced in this section to derive the theta Neuron model from Morris-Lecar model.

### 3.5.1 Hodgkin Classification of neural excitability

Even before bifurcation theory was developed, Hodgkin gave a classification for neurons. He classified neurons into the following two classes based on his electrophysiological experiments on the axon of squid neuron. He stimulated a cell with current of different strengths and made measurements of emerging frequencies of the action potential and on the basis of his recordings he made the following classifications[27]:

**Type I neural excitability:** The frequency of action potential increases with increasing applied current. It is possible to generate action potentials with arbitrarily low frequencies.

**Type II neural excitability:** The frequency of the action potential is insensitive to changes in the applied current.

Fig(3.4) shows the input to frequency response curves of type I and type II neural models. Hodgkin’s classification went unnoticed until Rinzel and Ermentrout published their work in 1989[28]. They treated the input current in neuronal models as a bifurcation

parameter. As the input current is increased a bifurcation is induced and the type of bifurcation determines the type of excitability. Type I corresponds to saddle-node on invariant circle bifurcation. When the input current crosses the threshold value, the neuron starts to fire. The frequency of firing changes with change in the input current. Hence the model of this class are known as integrators. The Morris-Lecar model and the theta neuron model are examples of this class. In Type II the underlying bifurcation is Andronov-Hopf. The frequency of firing is insensitive to change in input current. Such type of neurons fire only in a certain frequency band and therefore these are called resonators. The Hodgkin- Huxley models is an example of this class.

Although electrophysiologically there can be several mechanisms for excitability and spiking, there are however only four generic bifurcations a system can undergo in the absence of any additional constraints[9], [20].

### 3.5.2 Review of some relevent codimension 1 bifurcations

#### Saddle-node bifurcation

The normal form equation in 1-D for this type of bifurcation is

$$\dot{y} = \beta + y^2 \quad (3.8)$$

where  $\beta$  is the bifurcation parameter. For  $\beta < 0$  we have two fixed points one stable and another unstable , as  $\beta$  is increased to  $\beta > 0$  through  $\beta = 0$  these two fixed points coalesce and annihilate each other. We can clearly distinguish the two states as the resting state ( $\beta < 0$ ) and spiking state ( $\beta > 0$ ). Hence we can model the neuron's dynamical property of excitability and spiking using this model equation.

#### Saddle-node bifurcation on an invariant circle

Performing the transformation of variables  $y = \tan(\theta/2)$  in the Esq(3.8) then one obtains the following equation

$$\dot{\theta} = (1 - \cos(\theta)) + \beta(1 + \cos(\theta)) \quad (3.9)$$

This is the normal form equation for a saddle-node bifurcation on an invariant circle (SONIC) .This particular equation also represents the theta neuron model which is also the model we have used in our study. It is very much similar to saddle-node bifurcation

except that now the bifurcation occurs on an invariant circle i.e coalescing and annihilation of fixed points occurs on an invariant circle with emergence of limit cycle attractor for  $\beta > 0$ [8],[29].

### Supercritical Andronov-Hopf bifurcation

The Andronov-Hopf bifurcation occurs in two or higher dimensional systems. The normal form equation for the supercritical Andronov-Hopf bifurcation is as follows:

$$\begin{aligned}\dot{r} &= \mu r - r^3 \\ \dot{\theta} &= \omega + br^2\end{aligned}\tag{3.10}$$

where  $\mu$  is the bifurcation parameter,  $\omega$  is the frequency of the limit cycle and  $b$  relates the frequency to the amplitude in the case of large amplitudes. Here we have a stable fixed point (stable spiral) for  $\mu < 0$  which gets transformed into unstable spiral surrounded by limit cycle as  $\mu$  becomes greater than 0 . The effect of increasing  $\mu$  will be that the amplitude of the limit cycle will increase[30].

### Subcritical Andronov-Hopf bifurcation

The normal form equation for this case is

$$\begin{aligned}\dot{r} &= \mu r + r^3 - r^5 \\ \dot{\theta} &= \omega + br^2\end{aligned}\tag{3.11}$$

In this case for  $\mu < 0$  there are two attractors one a unstable limit cycle and a stable fixed point at origin. As  $\mu$  becomes 0 the unstable limit cycle shrinks to zero amplitude and turns the stable fixed point at origin into unstable fixed point. Now for  $\mu > 0$  we have a large amplitude stable limit cycle and a unstable fixed point at the origin[30].

## 3.6 Theta Neuron model

The theta neuron model is represented by canonical form equation of type-I excitability. A model is called canonical for a family of dynamical systems if every member of that family can be transformed by piecewise continuous possibly invertible change of variables. The usefulness of working with canonical models lies in the fact that they can mimic

the dynamical behaviour of the whole family[9]. In this section first we will review the reduction of the Morris–Lecar model to the theta neuron model and then we will review the dynamical properties of this model following ref.[8],[31],[32]. Let us write Eq(3.6) as follows,

$$\begin{aligned}\frac{dV}{dt} &= I + g_1(V, w) \\ \frac{dw}{dt} &= g_2(V, w)\end{aligned}\quad (3.12)$$

where  $g_i(V, w)$  corresponds to the nonlinear term on the right hand side of Eq(3.6). This can be written in matrix form by defining vector  $\mathbf{Z} = (V, w)^T$ . Let  $I_o$  be the critical value of the current for saddle node bifurcation in Morris-Lecar model and  $\mathbf{Z}_o$  be the corresponding point where a saddle node appears. Decomposing current  $I$  as  $I = I_o + \epsilon^2 \Delta I$ , where  $\epsilon$  is a small parameter. Eq(3.12) can be written as,

$$\frac{d\mathbf{Z}}{dt} = G(\mathbf{Z}) + \epsilon^2 \Delta I \begin{pmatrix} 1 \\ 0 \end{pmatrix}\quad (3.13)$$

where

$$G(\mathbf{Z}) = \begin{pmatrix} I_o + g_1(V, w) \\ g_2(V, w) \end{pmatrix}$$

Performing a Taylor's expansion of  $G(\mathbf{Z})$  around  $(\mathbf{Z} = \mathbf{Z}_o + \epsilon z(t)\mathbf{e})$  where  $\mathbf{e}$  is the unit eigen vector corresponding to zero eigen value of the Jacobian  $D_{\mathbf{Z}}(G(\mathbf{Z}))$  of  $\mathbf{G}$  at  $\mathbf{Z}_o$ .

$$G(\mathbf{Z}) = G(\mathbf{Z}_o) + D_{\mathbf{Z}}(G(\mathbf{Z}_o))^T \epsilon z \mathbf{e} + \mathbf{e}^T D^2_{\mathbf{Z}}(G(\mathbf{Z}_o)) \mathbf{e} \epsilon^2 z^2 + \dots$$

Substituting the above Taylor's expansion in Eq(3.13) we get

$$\epsilon \mathbf{e} \frac{dz}{dt} = G(\mathbf{Z}_o) + D_{\mathbf{Z}}(G(\mathbf{Z}_o))^T \epsilon z \mathbf{e} + \mathbf{e}^T D^2_{\mathbf{Z}}(G(\mathbf{Z}_o)) \mathbf{e} \epsilon^2 z^2 + \epsilon^2 \Delta I \begin{pmatrix} 1 \\ 0 \end{pmatrix} + \dots\quad (3.14)$$

Let  $\mathbf{f}$  denote a the left eigenvector such that  $\mathbf{f} \cdot \mathbf{e} = 1$ . Now on projecting Eq(3.15) on to  $\mathbf{f}$  one gets.

$$\epsilon \frac{dz}{dt} = \mathbf{f} \cdot \mathbf{e}^T D^2_{\mathbf{Z}}(G(\mathbf{Z}_o)) \mathbf{e} \epsilon^2 z^2 + \epsilon^2 \Delta I \mathbf{f} \cdot \begin{pmatrix} 1 \\ 0 \end{pmatrix} + \dots\quad (3.15)$$

Since the saddle node occurs at  $\mathbf{Z} = \mathbf{Z}_o$ ,  $G(\mathbf{Z}_o) = 0$  and also  $\mathbf{f} D_{\mathbf{Z}}(G(\mathbf{Z}_o))^T \mathbf{e} = 0$ . We can define two quantities  $\beta$  and  $q$  as follows:  $\beta = \Delta I \mathbf{f} \cdot \begin{pmatrix} 1 \\ 0 \end{pmatrix}$  and  $q = \mathbf{f} \cdot \mathbf{e}^T D^2_{\mathbf{Z}}(G(\mathbf{Z}_o)) \mathbf{e}$ .

Then Eq(3.15) can be rewritten as

$$\frac{dz}{dt} = \epsilon(\beta + qz^2) \quad (3.16)$$

Which is the normal form equation for saddle node bifurcation .We can get the theta neuron equation from this by carrying out the following transformation  $z = \tan(\theta/2)$  and  $\tau = \epsilon t$ , so Eq(3.16) becomes

$$\frac{d\theta}{d\tau} = q(1 - \cos \theta) + \beta(1 + \cos \theta) \quad (3.17)$$

We have therefore a normal form equation for a type-I neuron in the form of “phase equation” with  $\theta \in [0, 2\pi]$ ,  $\theta(0) = \theta(2\pi)$ . In our simulations we have taken  $q$  to be unity unity[31],[32]. Dimensionally,  $q$  and  $\beta$  are related to time scales, and the time scale of the membrane potential turns out to be in milliseconds when  $q = 1$  and  $\beta \ll 1$ . For sake of convenience of notation, we drop the symbol  $\tau$  for time and use  $t$  instead in Eq(3.17).

$$\frac{d\theta}{dt} = (1 - \cos \theta) + \beta(1 + \cos \theta) \quad (3.18)$$

The Eq(??) has two fixed points for  $\beta < 0$ .

$$\theta^\pm = \pm \cos^{-1}\left(\frac{1 + \beta}{1 - \beta}\right)$$

As  $\beta$  is increased these two fixed points moves towards each other and coalesce at  $\beta = 0$  and a saddle node bifurcation occurs. When  $\beta > 0$  there are no fixed point. Thus, a neuron can be represented by a point moving on unit circle  $S^1$ .

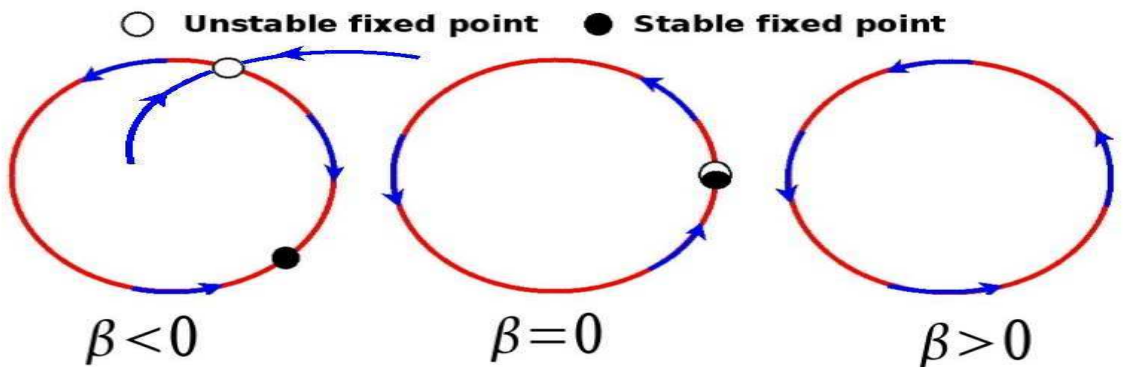


Figure 3.5: Bifurcation structure of theta neuron

### 3.7 Coupled Theta Neurons

A network of  $N$  coupled theta neurons is given by the equations

$$\frac{d\theta_i}{dt} = (1 - \cos \theta_i) + (\beta_i + \sum_{j=1}^N \alpha_j g_{ji} s_{ji})(1 + \cos \theta_i) \quad (3.19)$$

where  $\beta_i$  denotes the input current to the  $i^{\text{th}}$  neuron.  $\alpha_i$  is a constant and it represents the type of synapse. Its value is  $+1$  for excitatory and  $-1$  for inhibitory synapse.  $g_{ji}$  is the measure of coupling strength from the neuron  $i$  to neuron  $j$ . Please note that we have taken  $g_{ij} = 0$  for  $i = j$  in all of our simulations. The dynamics of synaptic conductances are modelled by the gating variable  $s_{ji}$ .

There are many ways to model synaptic conductances. In our simulations we have used an ordinary differential equation to model them. The coupling presented here is modelled under the assumption that synaptic transmission is also on the same time scale as the spikes. The value of  $s_{ji}$  remains between 0 and 1. As the neuron  $j$  spikes, its output jumps to 1 and then it slowly decays to 0. This decay is governed by the ordinary differential equation of the form

$$\frac{ds_{ji}}{dt} = -\frac{s_{ji}}{\tau_{ji}}$$

where  $\tau_{ji}$  is decay constant. This model of synaptic conductances is not physiologically adequate. Numerically as well it creates problems when jumps occur in  $s_{ji}$ . Therefore we add one more term to the above equation. This term takes into consideration the output of the presynaptic neuron and synaptic rise time. So we have the following ODE governing the time evolution of the gating variable[31].

$$\frac{ds_{ji}}{dt} = -\frac{s_{ji}}{\tau_{ji}} + e^{-\eta(1+\cos \theta_j)} \frac{1 - s_{ji}}{\tau_R} \quad (3.20)$$

Through this equation we are able to replace the jumps by rapid smooth rise. This makes numerical simulation of the synaptic conductances easier. The eq(3.20) also enables automatic regeneration of the next spike once the earlier has died down. So, in a system of two coupled theta neurons we will have two feedback equations via the gating variables  $s_{12}$  and  $s_{21}$ .

To model the output of the theta neuron as close as possible to the membrane potential of real neurons we have defined the neuron output as [33],[5],[6],[7]

$$x_i = 0.5(1 - \cos \theta_i) \quad (3.21)$$

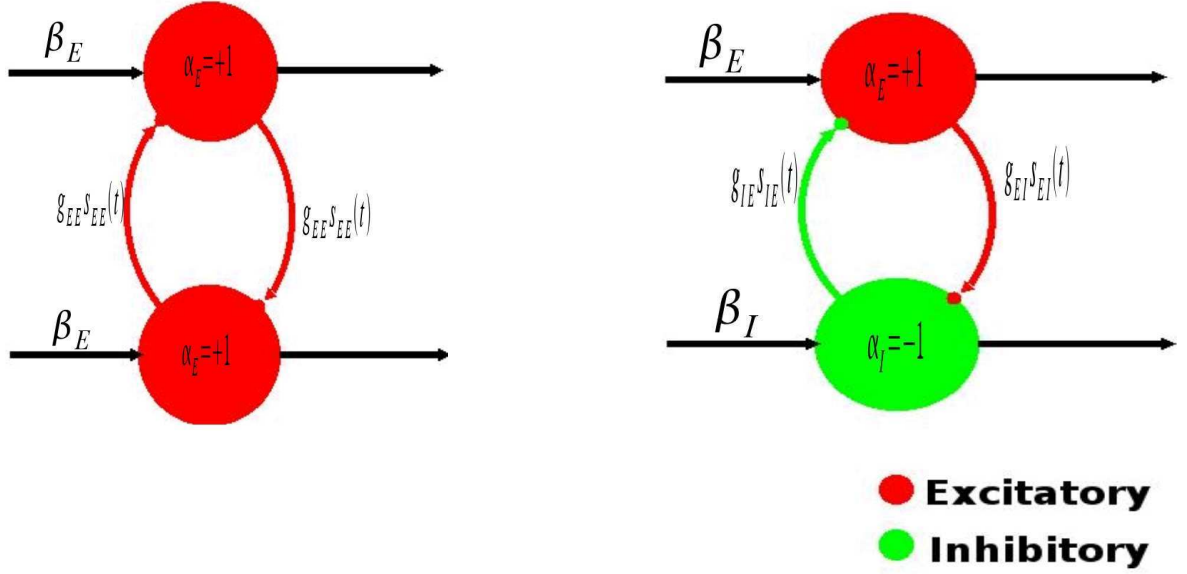


Figure 3.6: Bidirectional Coupling between two theta neurons. Left :excitatory - excitatory (E-E) type coupling , Right :inhibitory - excitatory (I-E) type coupling

Figures (3.7) to (3.9) are plots of some sample times series for the kind of connections shown in the Fig(3.6). For E-E case we have taken the following values of parameters  $\alpha_1 = 1, \alpha_2 = 1, g_{12} = g_{21} = 0.3, \tau_{12} = \tau_{21} = 2.0, \tau_R = 0.1, \eta = 5.0$  and  $\beta_1 = \beta_2 = 0.01$  and the initial conditions are  $\theta_1 = 0.0, \theta_2 = 0.01, s_{12} = 0.0, s_{21} = 0.0$ . We have used finite step size Runge-Kuta Fourth Order(RK-4) with time step  $h = 0.01$  to solve the above coupled differential equations numerically. We have generated a data set for 300,000 iterations. In the figures we show the end part of the time series after the transients have died down. For the I-E case we have taken the following values of parameters  $\alpha_1 = 1, \alpha_2 = -1, g_{12} = g_{21} = 0.3, \tau_{12} = 2.0, \tau_{21} = 10.0, \tau_R = 0.1, \eta = 5.0$  and  $\beta_1 = \beta_2 = 0.01$  and the initial conditions are  $\theta_1 = 0.0, \theta_2 = 0.01, s_{12} = 0.0, s_{21} = 0.0$ . A important observation is that in IE case for these values of parameters the excitatory neuron are not firing maximally i.e inhibitory neurons successfully able to inhibit the output of excitatory neuron. The time evolution of  $s_{21}$  looks like relaxation oscillations.

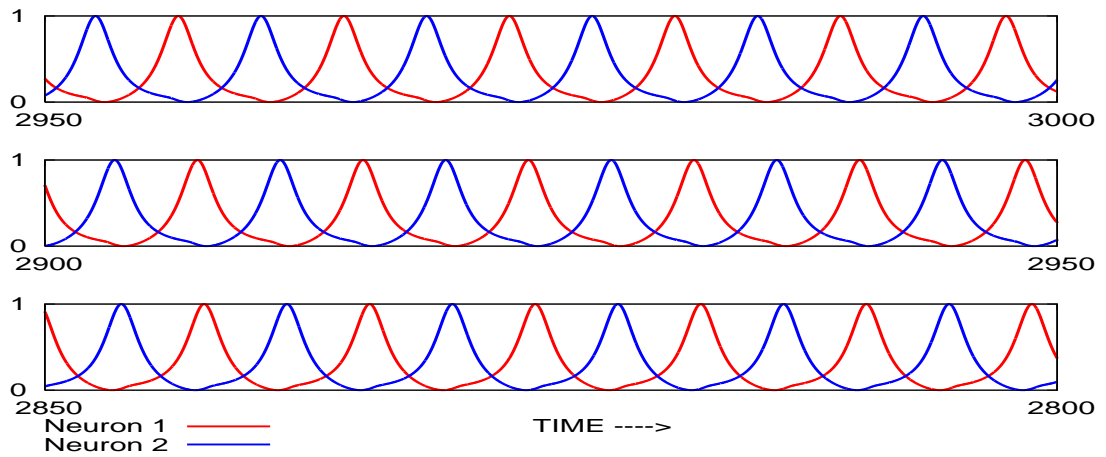


Figure 3.7: Time Series for EE case

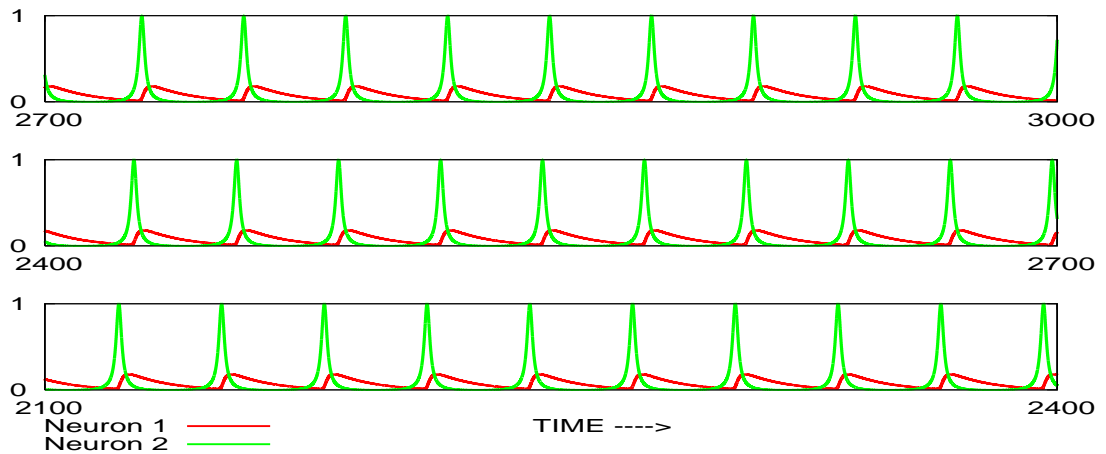


Figure 3.8: Time Series for IE case, Neuron 2 (green) is inhibitory and Neuron 1 (red) excitatory

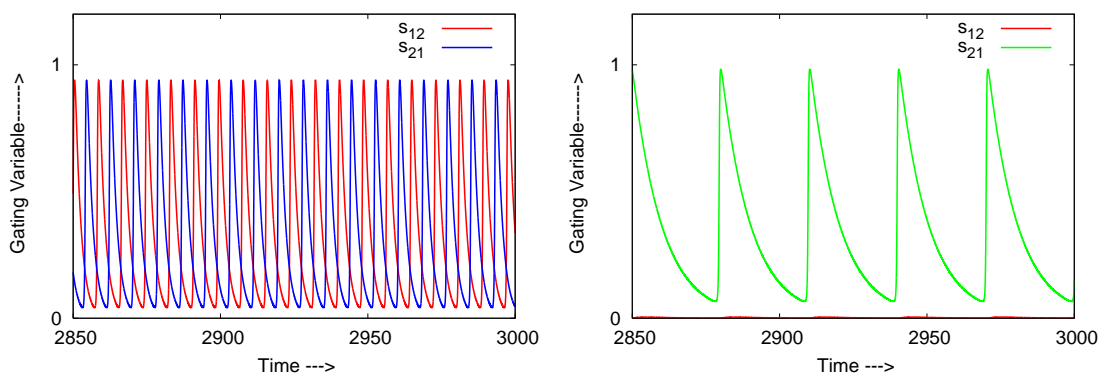


Figure 3.9: Gating variable  $s_{12}$  and  $s_{21}$  plotted for the above time series, Left: EE case, Right: IE case

## 3.8 Dynamics of a pair of coupled Theta Neurons

### Stability Analysis

We try to do a stability analysis of the system of equations governing the coupled theta neuron. Defining new variable  $x_i = 0.5(1 - \cos \theta_i)$  and then rewriting equations Eq(4.1) and Eq(3.20) in terms of the  $x_i$ 's for a pair of neurons the following four equations.

$$\begin{aligned} \dot{x}_1 &= (x_1 + (\beta_1 + \alpha_2 g_{21} s_{21}))(1 - x_1) \sqrt{1 - (1 - 2x_1)^2} \\ \dot{x}_2 &= (x_2 + (\beta_1 + \alpha_2 g_{21} s_{21}))(1 - x_2) \sqrt{1 - (1 - 2x_2)^2} \\ \dot{s}_{12} &= -\frac{s_{12}}{\tau_{12}} + \exp(-2\eta(1 - x_1)) \frac{(1 - s_{12})}{\tau_R} \\ \dot{s}_{21} &= -\frac{s_{21}}{\tau_{21}} + \exp(-2\eta(1 - x_2)) \frac{(1 - s_{21})}{\tau_R} \end{aligned} \quad (3.22)$$

First we try to find out the fixed points  $(x_1, x_2, s_{12}, s_{21})$  of the above system of equations. Let us define  $a_{ij} = \frac{\tau_{ij}}{\tau_R + \tau_{ij}}$ ,  $b_{ij} = \frac{\tau_{ij}}{\tau_R e^{2\eta} + \tau_{ij}}$ ,  $c_{ij} = \frac{\beta_j + \alpha_i g_{ij} a_{ij}}{\beta_j + \alpha_i g_{ij} a_{ij} - 1}$  and  $d_{ij} = \frac{\beta_j + \alpha_i g_{ij} b_{ij}}{\beta_j + \alpha_i g_{ij} b_{ij} - 1}$ . Then fixed point can be written in terms of  $a_{ij}$ ,  $b_{ij}$ ,  $c_{ij}$  and  $d_{ij}$  as follows:

$$\begin{aligned} &(1, 1, a_{12}, a_{21}), (0, 0, b_{12}, b_{21}), (1, 0, a_{12}, b_{21}), (0, 1, b_{12}, a_{21}), \\ &(1, c_{12}, a_{12}, \frac{\tau_{21}}{\tau_R \exp[2\eta(1 - c_{12})] + \tau_{21}}), (0, d_{12}, b_{12}, \frac{\tau_{21}}{\tau_R \exp[2\eta(1 - d_{12})] + \tau_{21}}) \\ &(c_{21}, 1, \frac{\tau_{21}}{\tau_R \exp[2\eta(1 - c_{21})] + \tau_{21}}, a_{21}), (d_{21}, 0, \frac{\tau_{21}}{\tau_R \exp[2\eta(1 - d_{12})] + \tau_{21}}, b_{21}) \end{aligned}$$

These fixed points defy bifurcation analysis as the elements of the Jacobian blow up. Apart from the above fixed points, other fixed point exist which are roots of the following system of coupled equations.

$$\begin{aligned} x_1 &= \frac{\beta_1 + \alpha_2 g_{21} s_{21}}{\beta_1 + \alpha_2 g_{21} s_{21} - 1} \\ s_{21} &= \frac{\tau_{21}}{\tau_R \exp[-2\eta(1 - x_1)] + \tau_{21}} \end{aligned} \quad (3.23)$$

and similarly of the system:

$$\begin{aligned} x_2 &= \frac{\beta_2 + \alpha_1 g_{12} s_{12}}{\beta_2 + \alpha_1 g_{12} s_{12} - 1} \\ s_{12} &= \frac{\tau_{12}}{\tau_R \exp[-2\eta(1 - x_2)] + \tau_{12}} \end{aligned} \quad (3.24)$$

the above equations are transcendental and cannot be solved analytically: Even if a numerical approach is taken, these have a continuous dependence on the values of the parameters. Hence a local bifurcation analysis is difficult for this system, if not impossible. To get over this problem and to understand the dynamics of the system we take a different approach and try to analyze it using other numerical techniques which follow this section.

## Frequency-Input curves and Lyapunov exponents

We take look at some more aspects of the dynamics of a pair of coupled theta neurons through frequency-input curves and Lyapunov exponents. In first case Fig(3.10) we have a EE system of bidirectionally coupled theta neurons and what we get is typical frequency-input curve, the only difference being that even at  $\beta = 0.0$  there is net frequency of firing. It is happens because now the bifurcation parameter is  $I_i$ , the input for  $i^{th}$  neuron and is given by

$$I_i = \beta_i + \sum_{j=1}^N \alpha_j g_{ji} s_{ji} \quad (3.25)$$

As noted earlier we take  $g_{ij} = 0$  for  $i = j$ . Hence now we have some net positive input going into the system due to the presence of second term  $\alpha_j g_{ji} s_{ji}$ . Both the frequency-input curve and the lyapunov exponents indicate that for this set of parameter values [refer:table(3.1)] the system is periodic with the presence of only a single frequency. In the next case Fig(3.11) we have again taken bidirectionally coupled EE theta neurons but with slightly different coupling strengths. In this case we see that there are two frequencies in the system after  $\beta$  crosses a value of approximately 0.7 at the same point in the lyapunov exponent curve and that the second largest lyapunov exponent also become zero, indicating the presence of second frequency in the system. So we can say that as the value of  $\beta$  is changed in this case, it makes a transition from a periodic to a quasiperiodic state. In the third and last case we consider IE type system with bidirectional coupling, the results being shown in Fig(3.12). Here we see that for small values of  $\beta$  there are a lot of fluctuations in the frequency of the excitatory neuron. Similar fluctuations are

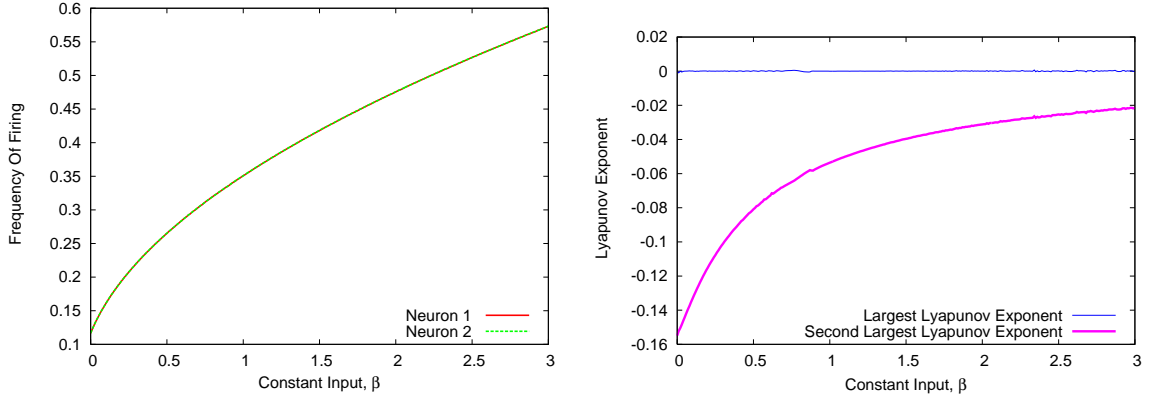


Figure 3.10:

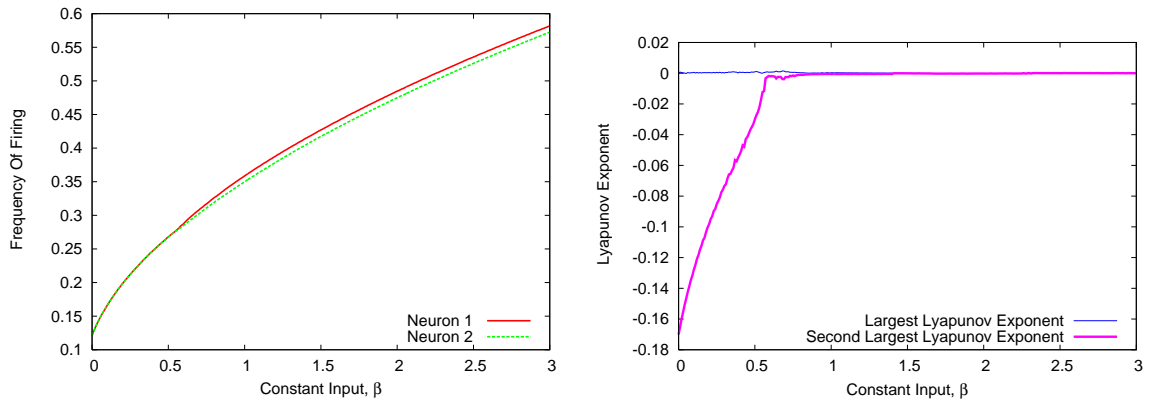


Figure 3.11:

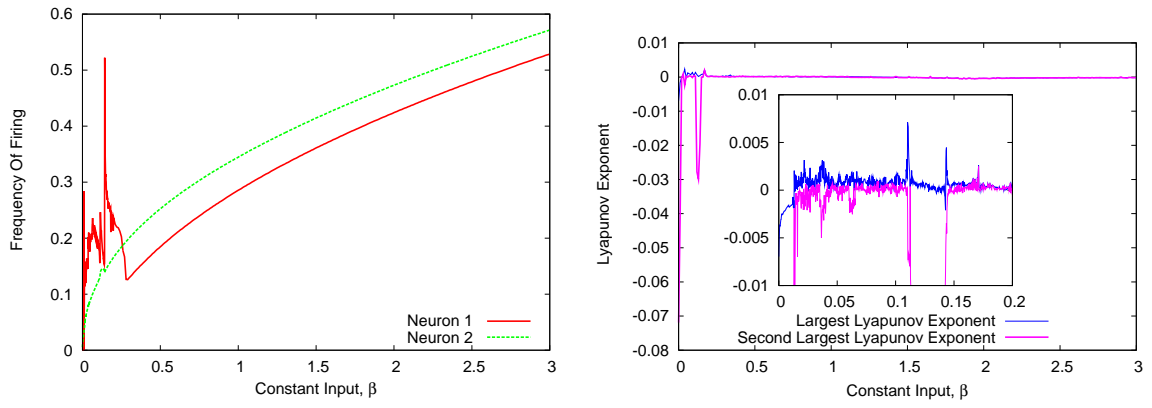


Figure 3.12:

Figure.No.	$g_{12}$	$g_{21}$	$\tau_{12}$	$\tau_{21}$	$\alpha_1$	$\alpha_2$	$\eta$	$\tau_R$
3.10	0.3	0.3	2.0	2.0	1	1	5.0	0.1
3.11	0.3	0.45	2.0	2.0	1	1	5.0	0.1
3.12	0.3	0.3	2.0	2.0	1	-1	5.0	0.1

Table 3.1: Values of parameters corresponding to the figures above the table

observed in the Lyapunov exponent curve also for small  $\beta$  (approx.  $\beta < 0.2$ , shown in the inset curve). These fluctuations are due to the bifurcation parameter oscillating between two regions. The stable region where  $I_i < 0$  and the unstable region  $I_i > 0$ . It might be possible that system is chaotic for some values of  $\beta < 0.2$ . The method followed in calculating Lyapunov exponent is given in the Appendix A.

## Bifurcation diagrams

We take a look at bifurcation diagrams, drawn very differently from the usual bifurcation diagrams drawn on an invariant circle. Since we are taking  $x_1$  and  $x_2$ , the membrane potentials for most of our analysis including the above Hilbert transform. So it is a better choice to draw bifurcation diagrams with them rather than with  $\theta_1$  and  $\theta_2$ . One more consideration in drawing them is to present the maximum possible information through them. We know that in saddle node bifurcation on an invariant circle the firing starts after  $\beta$ 's value crosses the threshold, which in our case is  $\beta = 0$ . Now on introducing the coupling, the bifurcation parameter is the time evolving input  $I$ . But still the parameters of the systems, i.e external input  $\beta$  and the couplings  $g_{12}, g_{21}$  are important to us and we can vary one of them keeping the other constant and see how the firing patterns change.

Fig(3.13) represents the case where we are keeping the coupling strength fixed at  $g_{12} = g_{21} = 0.3$ , the values of other parameters are  $\tau_{12} = 2.0, \tau_{21} = 2.0, \tau_R = 0.1$ . We observe that when  $\beta < 0$  there is no firing and when  $\beta > 0$  there is no firing. Similar diagram have been obtained for even the IE case also which we have shown below. In the Fig(3.16) we show the effect of changing coupling strengths. In the Fig(3.8) we vary  $g$ 's and in Fig(3.20) and Fig(3.21) we vary  $\tau$ 's. All the parameters are the same as in the previous cases except the changing the values of  $\alpha$ 's according to synapse type.

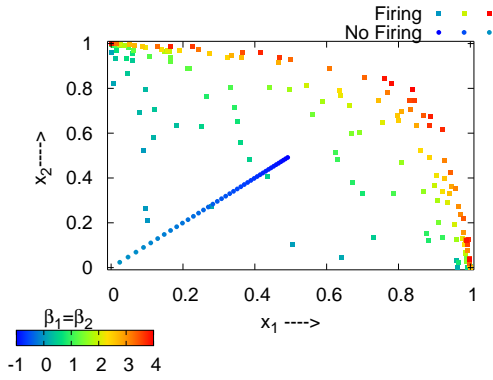


Figure 3.13: Bifurcation diagram for EE case

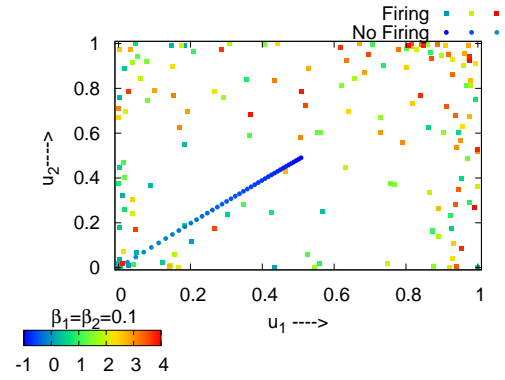


Figure 3.14: Bifurcation diagram for IE case

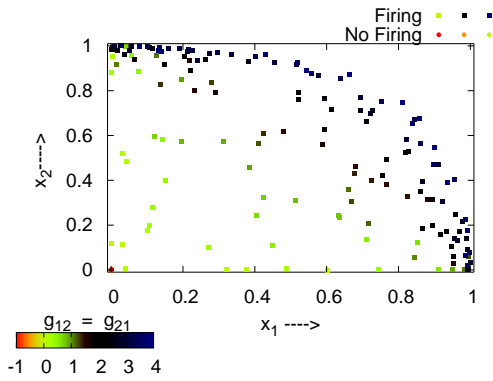


Figure 3.15: Effect on firing of change in coupling strength (EE case)

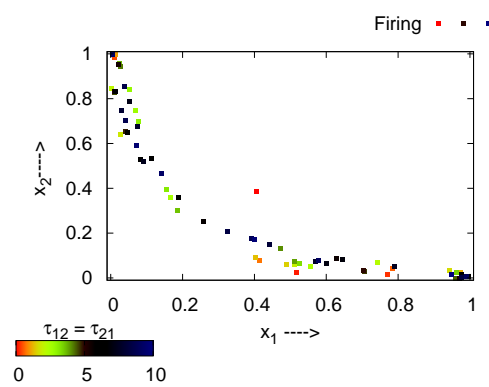


Figure 3.17: Effect on firing of change in decay constant  $\tau$  (EE case)

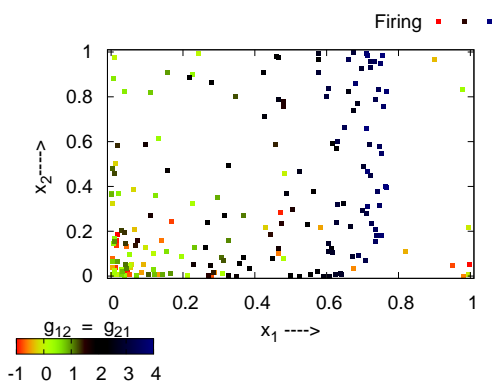


Figure 3.16: Effect on firing of change in coupling strength (IE case)

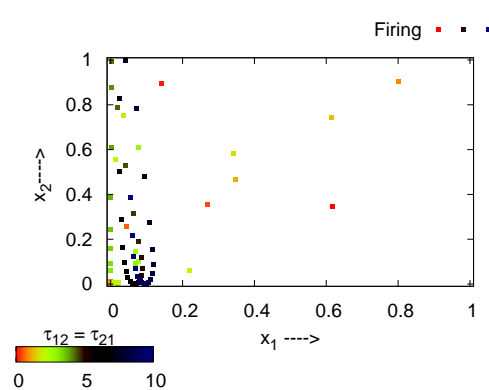


Figure 3.18: Effect on firing of change in decay constant  $\tau$  (IE case)

# Chapter 4

## Noise induced Synchronization and firing in coupled theta neuron

The game of science is, in principle, without end. He who decides one day that scientific statements do not call for any further test, and that they can be regarded as finally verified, retires from the game.

**Sir Karl Raimund Popper**

---

### 4.1 Introduction

As we have mentioned in the introduction, noise is inherent in biological systems and neurons are no exception to it. In this chapter we take a look at the effects induced by noise on a system of coupled theta neurons. Our main interest in the work presented is in noise induced transition to synchronization. Type I neurons are difficult to synchronize under deterministic conditions, so we look at whether noise can induce synchronization in a pair of coupled theta neurons. Considering different combinations of parameters involved in this system, we try to find out how synchronous activity takes place [5],[6],[7]. It is well known that inhibition leads to synchronization in deterministic systems [35],[31]. The model of coupled theta neurons we have studied also shows parameter regimes where there is collaborative activity between an inhibitory and an excitatory neuron. We have investigated the effect of the noise in these regimes.

## 4.2 Neuronal Noise

Neuronal noise is the term used for random influences on the transmembrane voltage of single neurons and by extension the firing activity of neural networks. It can affect firing activity of neurons and also can influence the transmission and integration of signals.

### Origin of neuronal noise

Among various sources constituting neuronal noise, the contribution from synaptic noise dominates. Fluctuations in the neurotransmitter level in the synapse constitute an important source of synaptic noise in the neuron. Chemical synapses don't work as deterministic switches but they convert a spike into a fixed packet of neurotransmitters which are released in the synaptic cleft. Synapses release neurotransmitters probabilistically and at times even without incoming spike. The real reason for this lies in the molecular events that precede the arrival of a spike at a synapse. The fluctuations in plasticity processes also influence the strength of a synapse and it is possible that they also have some contribution in overall synaptic noise[36]. But the dominant source of the synaptic noise is the synaptic bombardment of the inputs: There are huge number of synaptic connections on each neuron and each spike a neuron receives at its synapse adds some random current to the cell. Another source of neuronal noise are the conductance fluctuations in ion channels. There are two sources for these fluctuations, one is what is known as ion shot noise which is due to the variability in the amount of ions migrating into the cell or out of the cell when a channel is in its open state, thermal fluctuations constitute the other source.

### Modelling neuronal noise

Modelling neuronal noise involves the use of methods of stochastic dynamical systems. The modelling of neuronal noise basically depends on the source of the noise. Gaussian white noise is mainly used for modelling the internal sources of noise like thermal fluctuations etc. as the time scales involved in their production are much faster than the time scale of an action potential. Even though the synaptic noise production are at very slow time scales but as a single neuron has several thousands of synaptic connections, the cumulative effect of the fluctuations can be considered to be happening at faster time

scale, justifying the use of Gaussian white noise to model the neuronal noise.

## Effects of neuronal noise

Apart from assisting in synchronization, noise can induce many other effects in neurons. We mention a few below.

*Variability in firing*:- Presence of noise term in the neuron model will make it act as a stochastic oscillator. That is there will be variability in the firing pattern. If the neuron is quiescent (below threshold), noise can induce firing[5],[6],[7]. We will show this phenomenon in the theta neuron model in the next section.

*Stochastic Resonance* :- It is a phenomenon in which noise enhances the response of a nonlinear system to small external time-dependent forcing. A similar phenomenon is observed in neuronal models where a moderate amount of noise induces an output pattern that shows the strongest signature of the periodic input[37].

*Bursting*:- Neuronal bursting has a role in the way neurons encode information. A small noise can induce bursting in neuronal models[38].

### 4.3 Noise term in coupled theta neuron

Addition of Gaussian white noise on the right hand side of Eq(3.14) enters the theta neuron model multiplicatively as an input as follows:

$$\frac{d\theta_i}{dt} = (1 - \cos \theta_i) + (\beta_i + \sum_{j=1}^N \alpha_j g_{ji} s_{ji} + \sigma \xi(t))(1 + \cos \theta_i) \quad (4.1)$$

where  $\xi(t)$  is a Gaussian white noise with:

$$\langle \xi(t) \xi(t - \tau) \rangle = 2\delta(\tau). \quad (4.2)$$

and  $\sigma$  is the noise strength[39]. We interpret noise in the Stratonovich sense and integrate it with the time step  $h = 0.01$  using Stochastic RK-4(discussed in the Appendix C).

## 4.4 Noise induced firing in coupled theta neuron

As noted earlier, we find parameter regimes where inhibitory spike is able to inhibit the excitatory neuron completely [5],[6],[7]. We take another such parameter regime and try to find the effect of introducing small noise in the system. We show our result in Fig(4.1) and Fig(4.2). The values of the parameters take were as follows:-  $g_{12} = g_{21} = 0.25$ ,  $\tau_{12} = \tau_{21} = 2.0$ ,  $\tau_R = 0.1$ ,  $\eta = 5.0$  and  $\beta_1 = \beta_2 = 0.01$ . In the noise less case (Fig(4.1)) we

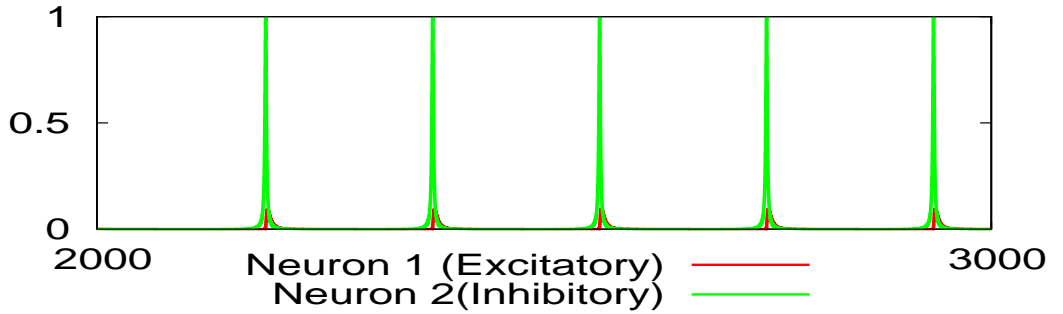


Figure 4.1: IE coupling, in absence of noise i.e  $\sigma = 0$

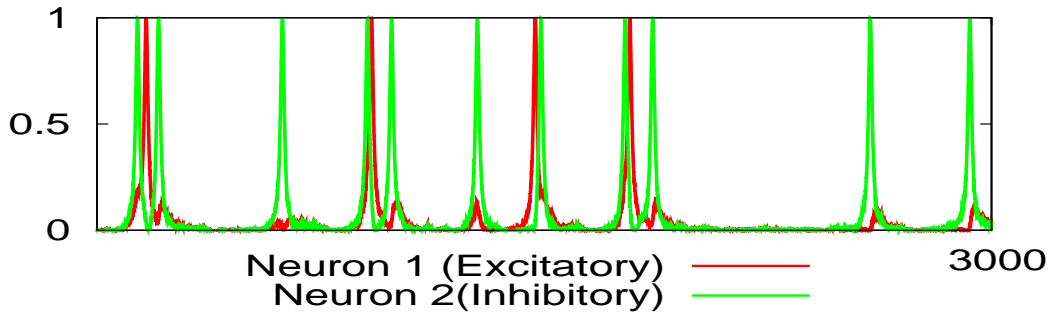


Figure 4.2: IE coupling, in presence of noise i.e  $\sigma = 0.025$

observe regular firing of the inhibitory neuron and the excitatory neuron does not fire at all. On introducing a little noise in to system ( $\sigma = 0.025$ ), the inhibitory neuron starts to fire irregularly and also the interesting observation is that now excitatory neuron also starts to fire. This happens because now the input of excitatory neuron is able to cross the threshold due the presence of a finite amount of noise in it. To understand this we rewrite the input which enters into theta neuron as below :

$$I_i = \beta_i + \sum_{j=1}^N \alpha_j g_{ji} s_{ji} + \sigma \xi(t) \quad (4.3)$$

When  $\beta_i = 0$  and  $\alpha_j = -1$  then  $I_i < 0$  for  $\sigma = 0.0$ , and this means the neuron is below the threshold of firing and hence in the absence of noise, excitatory neurons do not fire but as we introduce some finite noise, it starts to fire. In Fig(4.3) we show that the frequency of firing in the presence of noise is higher than in the noiseless case but as the external input  $\beta$  is increased, the effect of noise on the firing frequency dies down. We obtained similar results for EE case also.

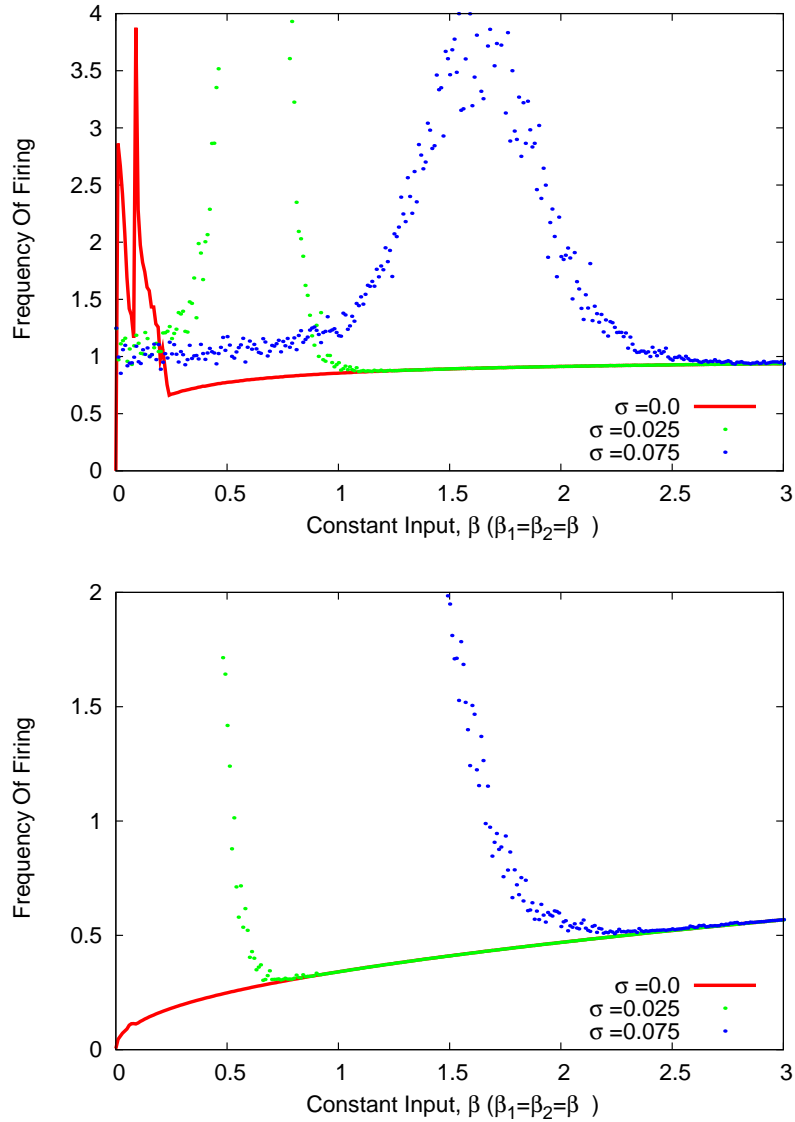


Figure 4.3: Frequency of firing and effect of noise on it for IE type coupling(Above:Excitatory neuron,Below:Inhibitory neuron)

## 4.5 Noise induced complete synchronization in coupled theta neurons

### Identical neurons

In this section we present our results on complete synchronization in theta neurons[5],[6],[7]. And also from our simulations we try to find out the factors which influence its stability. To observe complete synchronization we need to have identical systems. So we take two E-E coupled oscillators with identical parameters but different initial conditions. In the simulation we have taken  $g_{12} = g_{21} = 0.3$ ,  $\tau_{12} = \tau_{21} = 2.0$ ,  $\tau_R = 0.1$ ,  $\eta = 5.0$  and  $\beta_1 = \beta_2 = 0.1$ . We observe complete synchronization between the neurons at a noise strength  $\sigma = 0.301$ , i.e the time evolution of the two neurons become identical on introducing this much amount of noise Fig(4.4,4.5 , 4.7b). In figure(4.7a) we had noise strength little lesser i.e  $\sigma = 0.30$ , and the system does not get completely synchronized, but there is a large window of complete synchronization.

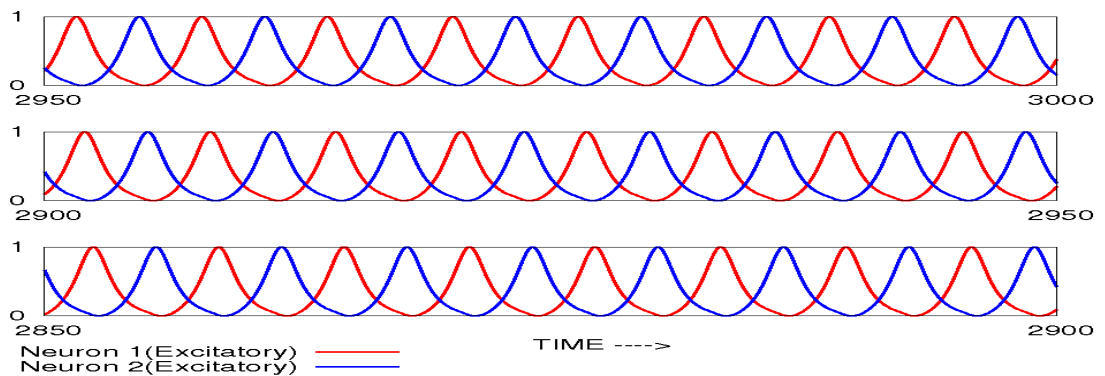


Figure 4.4: EE coupling, in absence of noise i.e  $\sigma = 0$

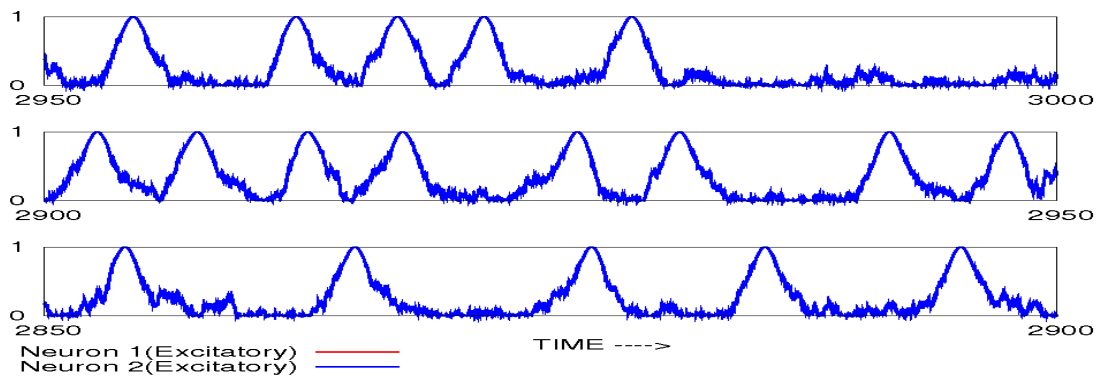


Figure 4.5: EE coupling, in presence of noise i.e  $\sigma = 0.301$

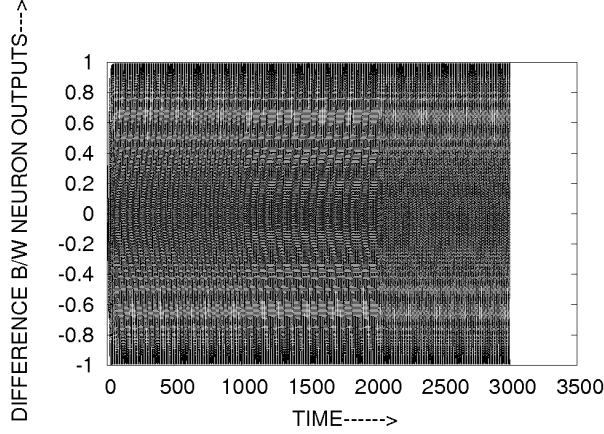


Figure 4.6: Output difference vs time for EE coupling in absence of noise  $\sigma = 0.0$ , below same curve at two different noise strengths

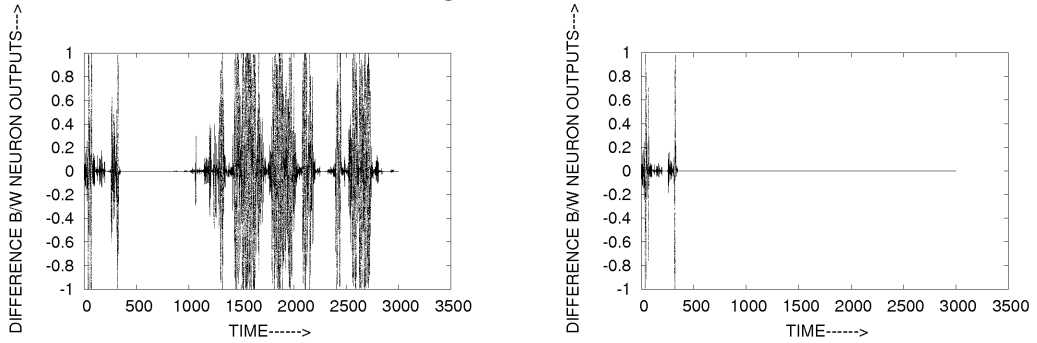


Figure 4.7: (a):  $\sigma = 0.30$

(b):  $\sigma = 0.301$

**Effect of coupling strength:-** We had seen complete synchronization above in which two systems started at different initial conditions but synchronized on introducing a noise of optimal strength. We calculate a quantity  $\langle |x_1 - x_2| \rangle$ , which is the average of modulus of output differences taken over all the iterations. We plot this quantity as a function of the coupling constant and the noise strength as shown in Fig(4.8) and Fig(4.9). We observe a transition from the synchronized state to the unsynchronized state as the coupling strength is increased for a particular noise strength. Also we see that a transition to synchronization at higher values of coupling strength occurs at higher noise strengths. There seems to be a functional relationship between coupling strength, noise and the quantity  $\langle |x_1 - x_2| \rangle$  [5],[6],[7].

**Effect of the external input:-** Here  $\langle |x_1 - x_2| \rangle$  is plotted as function of  $\beta$  and shown in Fig(4.10). The values of parameters and initial conditions are same as used in Fig(4.8) and Fig(4.9). The only difference is that now the quantity varied is  $\beta_1 = \beta_2 = \beta$  and coupling strengths are  $g_{12} = g_{21} = 0.3$ . We have varied  $\beta$  from 0 to 7, to see the whole

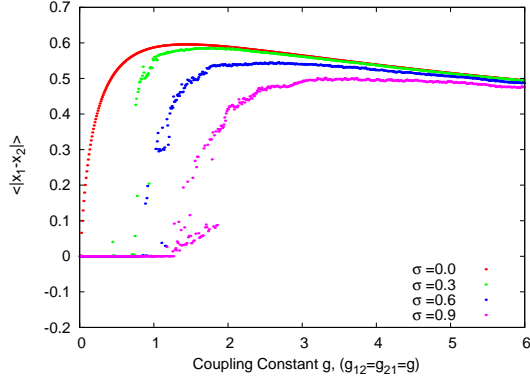


Figure 4.8: Noise strength vs  $\langle |x_1 - x_2| \rangle$  at different values of the coupling

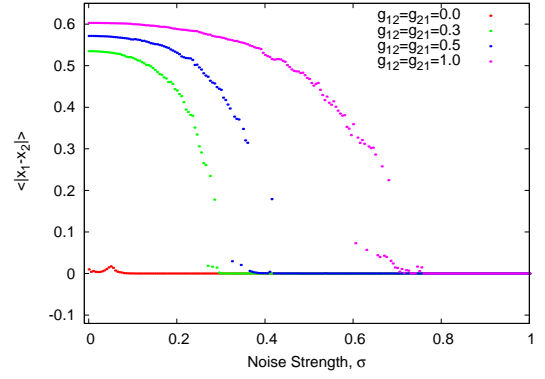


Figure 4.9: Coupling strength vs  $\langle |x_1 - x_2| \rangle$  at different values of the noise strength

parameter range. It is a little hard to make out much from this curve because as  $\beta$  is increased at lower noise values the system is fluctuating between the synchronized and unsynchronized state. But at the same time it should be noted that at a moderate noise strength of  $\sigma = 0.6$  the system is synchronized for whole of the regime of  $\beta$  shown in the curve.

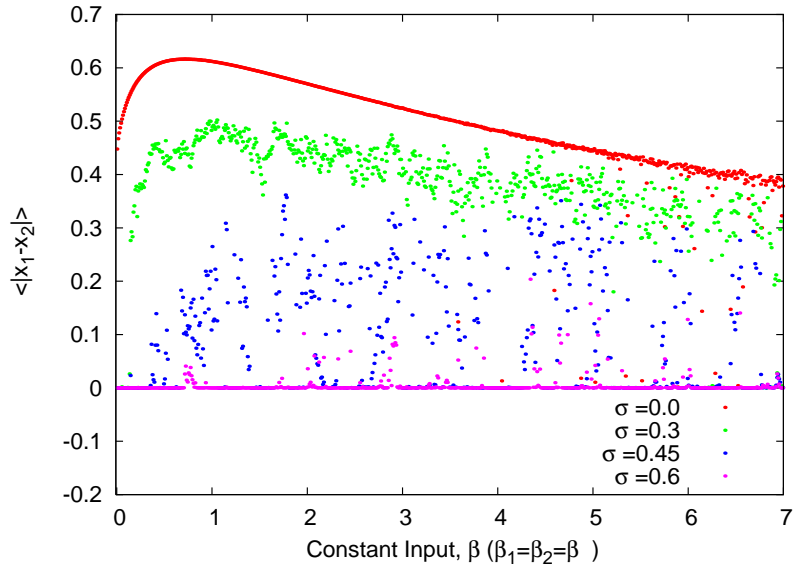


Figure 4.10: Input vs  $\langle |x_1 - x_2| \rangle$  at different values of the noise strength

We can also visualize the effect of change in input as shown in Fig(4.11) and Fig(4.12) [5],[6],[7]. Again in these curves also we see at strong noise, the system is synchronized even for very high values of  $\beta$ .

**Effect of noise strength:-** It is interesting to find out how noise strength affects the system if it is increased keeping all the parameters constant. In other words what is the difference between two values of noise strengths for both of which complete synchroniza-

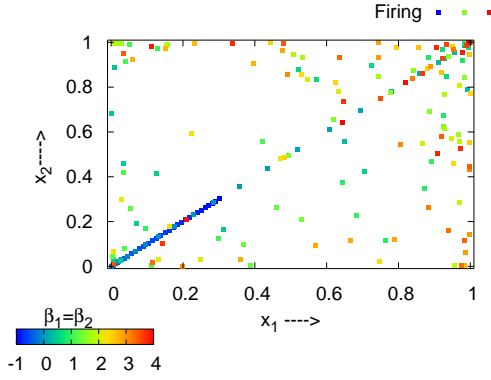


Figure 4.11: In presence of noise,  $\sigma = 0.375$

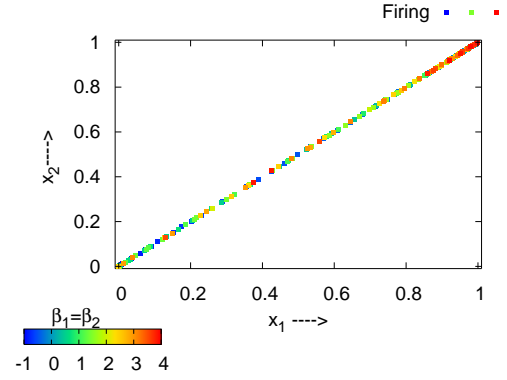


Figure 4.12: In presence of noise,  $\sigma = 1.0$

tion occurs. For this purpose we try to find out the time in which system synchronizes using the normal clock function available with C-programming language and measure the time. The result is plotted in the Fig(4.13) [5],[6],[7]. From the curve it is apparent that synchronization occurs faster as noise strength is increased.  $T_{syn}$  is the time the system takes to synchronize. It is clearly reducing as the noise strength is increasing.

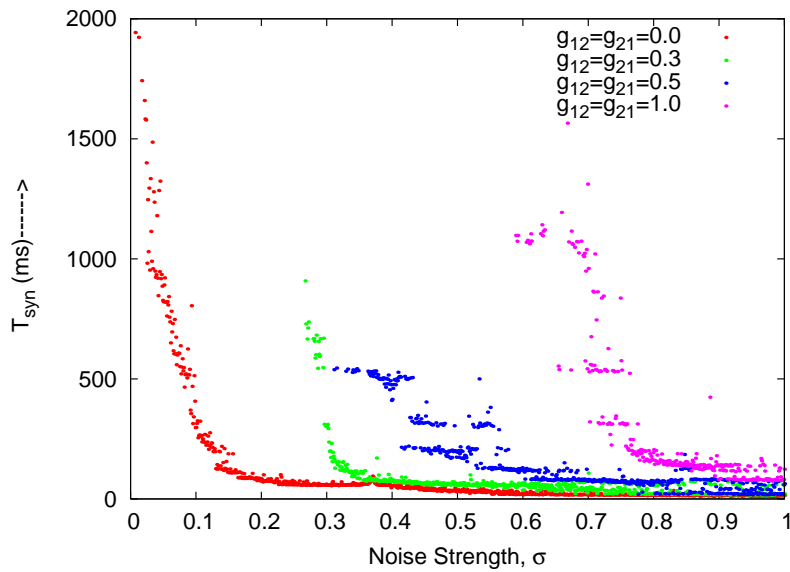


Figure 4.13: Effect of noise on rate of synchronization

## Lyapunov exponent in presence of noise

In the course of study of the system of coupled theta neurons, we calculated Lyapunov exponents. In Fig(4.14) and Fig(4.15) we have shown the curves of largest Lyapunov exponent in presence of noise [5],[6],[7]. This also, just as all other results in this dissertation, has not been published earlier in the available literature. The parameter used for

EE and IE cases were  $\beta_1 = \beta_2 = 0.1$ ,  $\tau_{12} = \tau_{21} = 2.0$ ,  $\tau_R = 0.1$ ,  $\eta = 5.0$ . In the both cases we observe that it becomes negative on adding noise. It is thought that a negative Lyapunov exponent in the presence of noise indicates synchronization in the system. But it is not a conclusive proof for predicting noise induced synchronization. However, it still seems that two identical excitatory neurons will undergo complete synchronization, as also two identical inhibitory neurons among themselves. In a simulation of 200 neurons in Section(4.8) we give a proof of this prediction. It is important to look at what happens in case of two nonidentical neurons, but we can't make any definite prediction based on presented calculation of Lyapunov exponents. Complete synchronization in a system of 200 nonidentical neurons has also been observed by us for the first time[5],[6],[7].

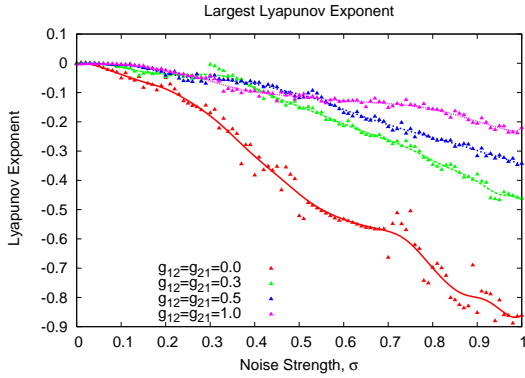


Figure 4.14: Lyapunov exponent in presence of noise for EE coupling

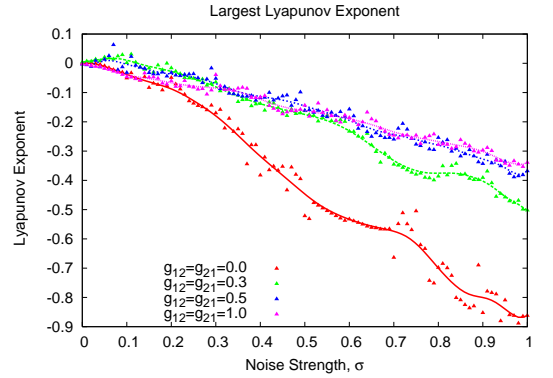


Figure 4.15: Lyapunov exponent in presence of noise for IE coupling

## Nonidentical neurons

We define nonidentical neurons as those for which any of the parameters involved are nonidentical including input  $\beta$ 's. We expect a system with different parameter values to have different dynamical behaviors and it becomes difficult to observe complete synchronization in such a system. According to our definition of nonidentical neurons the IE is nonidentical system, even though all the parameters except the synapse type ( $\alpha$ ) is different. Below we present a curve for the IE system with the following parameters  $g_{12} = g_{21} = 0.3$ ,  $\tau_{12} = \tau_{21} = 2.0$ ,  $\tau_R = 0.1$ ,  $\eta = 5.0$  and  $\beta_1 = \beta_2 = 0.0$ . We can clearly observe in figure(4.16) that rather than taking the system closer to a state of complete synchronization, noise is taking it away from it. But it is very much possible to observe CS in time windows even for some nonidentical coupled neurons also. We present one such

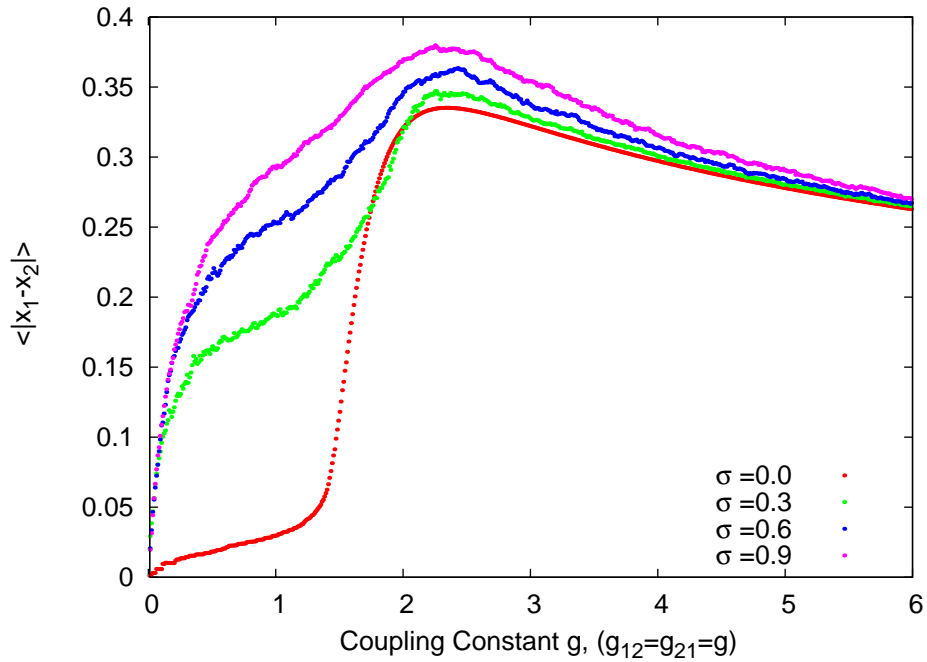


Figure 4.16: Effect of noise on IE system with varying coupling strength

simulation where this can be clearly seen in in Fig(4.17). In this simulation we have taken values of  $\beta$ 's which are little different,  $\beta_1 = 0.0001$  and  $\beta_2 = 0.0$  with other parameters being  $g_{12} = g_{21} = 0.3, \tau_{12} = \tau_{21} = 2.0, \tau_R = 0.1, \eta = 5.0$  and initial conditions were taken same. We observe bursts and resynchronizations of the system indicative of the fact that the transition to complete synchronization state is not stable.

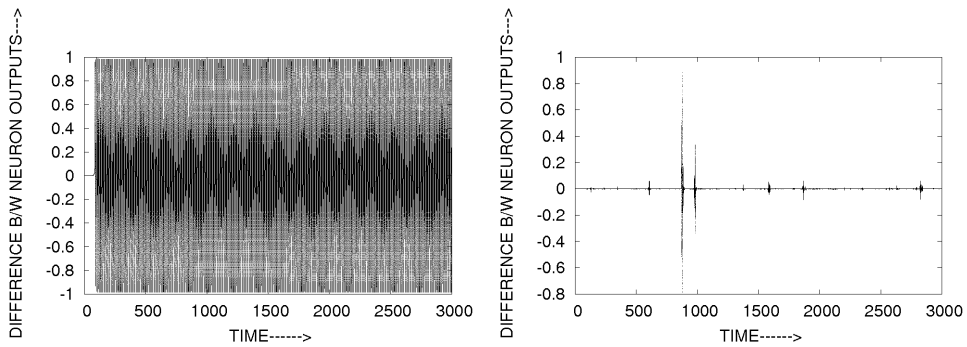


Figure 4.17: Right:Output difference in absence of noise,Left:Output difference in presence of noise( $\sigma = 0.75$ )

## 4.6 Instantaneous phase-frequency plots

We observed [5],[6],[7] that the plots between the instantaneous phase & instantaneous frequency of the inputs

$$I_i = \beta_i + \sum_{j=1}^N \alpha_j g_{ji} s_{ji} \quad (4.4)$$

going into each neuron gives information about whether the system would undergo complete synchronization or not. In the cases where complete synchronization occurs we observe structures as in the phase frequency plots of the Fig((4.20). It will be noted that the signature of complete synchronization is the almost identical nature of the plots for the two systems that are in synchrony, be it with or without noise. On the other hand, the absence of complete synchronization gets reflected in the non-identical phase–frequency plots for the input received by the neurons as shown in Fig(4.21). This is again true for both the noiseless as well as noisy cases[5],[6],[7].

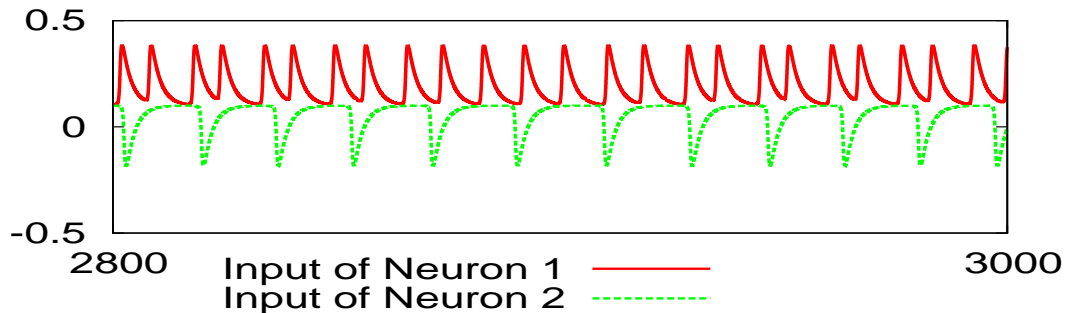


Figure 4.18: Time series of inputs to two neurons, showing relaxation oscillations

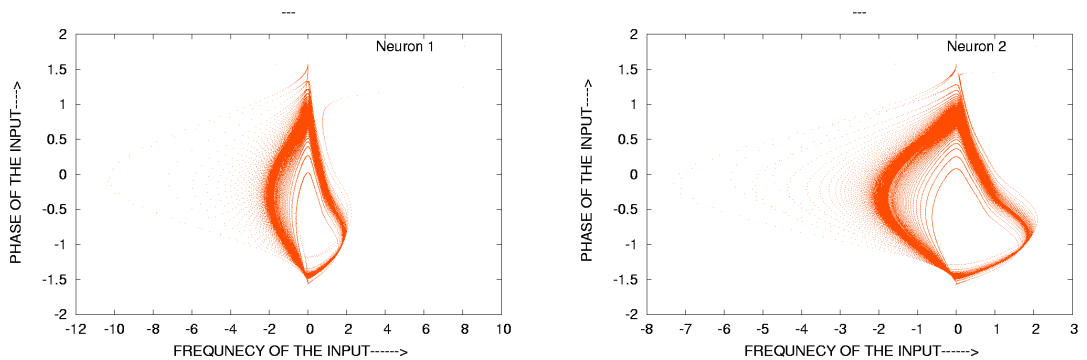


Figure 4.19: Curves between phase and frequency of the input  $I$

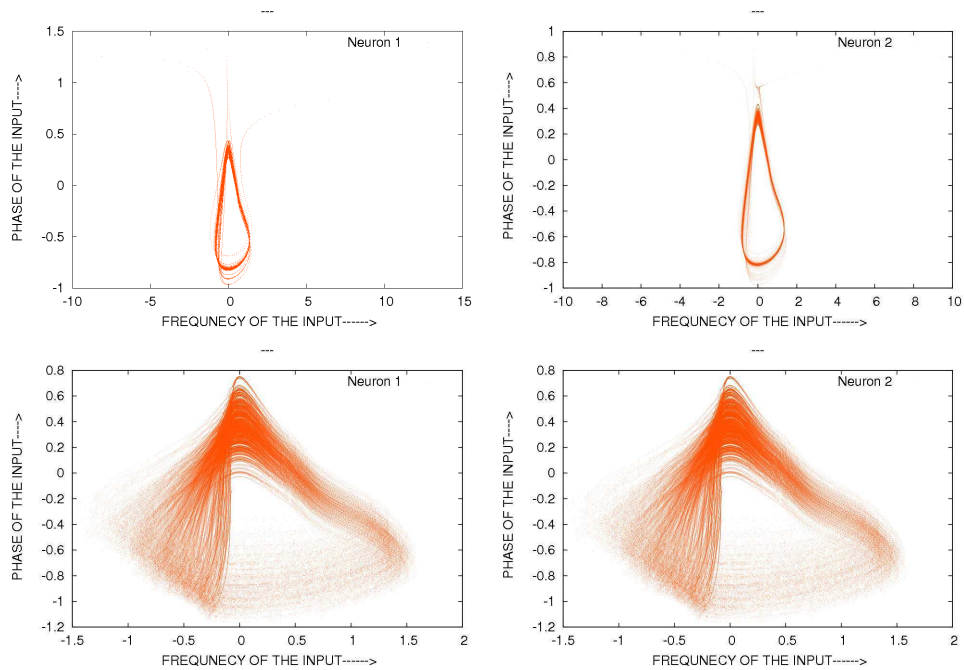


Figure 4.20: The upper panel of figures is the noise less case in lower panel we have noise of strength( $\sigma = 0.301$ ).

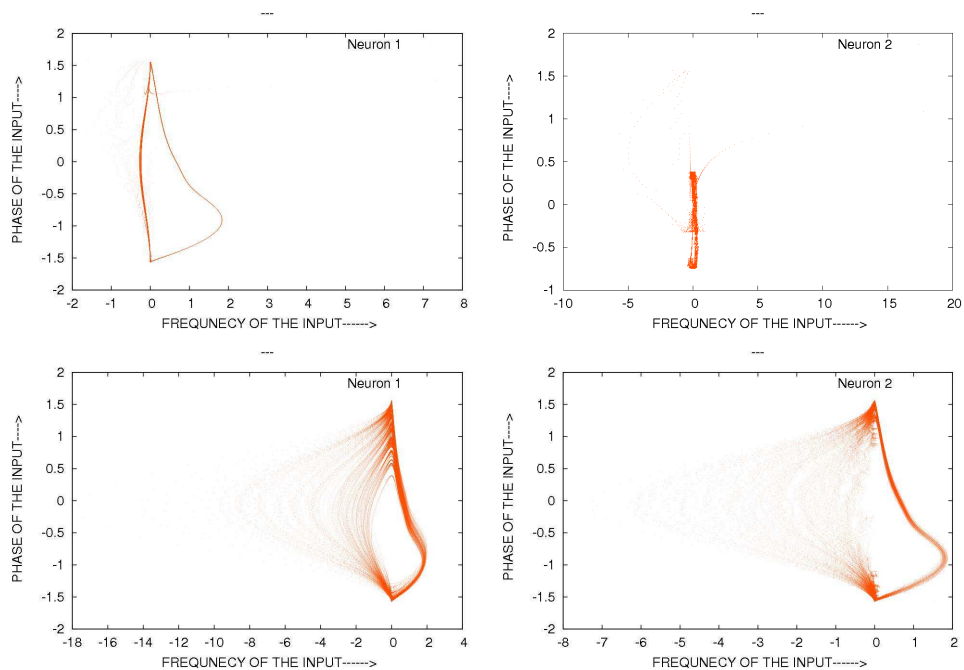


Figure 4.21: The upper panel of figures is the noise less case in lower panel we have noise of strength( $\sigma = 0.09$ ).

One striking feature of all these plots is their strange, flame like structures. The flame shape is reminiscent of canards that are typically associated with systems exhibiting relax-

ation oscillations or those showing transitions from small amplitude oscillatory motion to relaxation-oscillations as happens in the Belousov-Zhabotinsky reaction [34]. Though the flames may not be true canards, the time series for the neuronal inputs do show relaxation oscillations Fig(4.18) indicating a separation of time scales. There are two cases we are presenting — one in which we observe complete synchronization Fig(4.20). Parameters used in this EE case are  $\beta_1 = 0.1, \beta_2 = 0.1, g_{12} = g_{21} = 0.3, \tau_{12} = \tau_{21} = 2.0, \tau_R = 0.1, \eta = 5.0$ , and another one in which we haven't observed CS Fig(4.21,4.18). Parameters used in this IE case are  $\beta_1 = 0.0, \beta_2 = 0.0, g_{12} = g_{21} = 0.3, \tau_{12} = \tau_{21} = 2.0, \tau_R = 0.1, \eta = 5.0$ . CS was not observed in the case of the IE system even at very strong noise but in the above figures we see that at very little noise we are getting structures in input's phase and instantaneous frequency curves quite similar to each other even though the structures in noiseless case were very different from each other. This indicates there is some kind of order coming up in phase. We show in the next section that it is phase synchronization does happen in this case.

## 4.7 Noise induced phase synchronization in IE coupling

For this we take probably one of the most pathological case where all the parameters are different and try to see whether some kind of order is induced in phase. For this purpose we do a statistical interpretation of phase. The values of the parameters used are as follows  $g_{12} = g_{21} = 0.3, \tau_{12} = \tau_{21} = 2.0, \tau_R = 0.1, \eta = 5.0$  and  $\beta_1 = \beta_2 = 0.0$  and coupling type is IE. . The phase difference  $\Phi = \phi_1 - \phi_2$  where  $\phi_1$  and  $\phi_2$  are the phases of neuron 1 and 2 respectively. So, the condition  $\Phi \in [-\pi, \pi]$  is automatically satisfied on taking Hilbert Transform and then taking the phase difference. A peak in  $\Phi$  manifests as a preferred phase difference between the systems, if we interpret phase difference in statistical sense[40],[11]. In the presence of noise, this kind of coherence in phase difference is termed as phase synchronization. On increasing the strength of noise the peak is becoming sharper and sharper which means noise is able to induce more and more order in the phase.

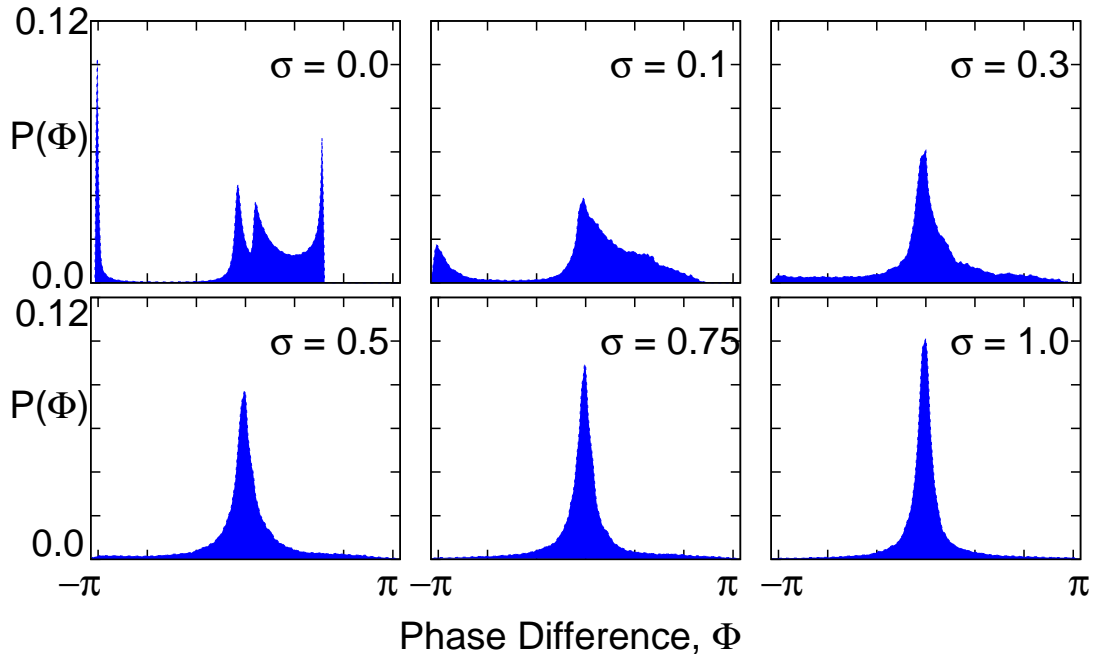


Figure 4.22: Effect of noise on rate of synchronization

## 4.8 A simulation of an ensemble of 200 neurons

In the first case we take an ensemble of 200 uncoupled theta neurons. All of them are receiving the inputs of the same strength i.e  $\beta = 0.1$ . The only difference between them is in the initial conditions,  $\theta_i(0) = r_1$  where  $r_1$  is a random number between 0 and  $2\pi$ . A noise of strength  $\sigma = 0.25$  is introduced into the system which results in complete synchronization. The outputs for this simulation is shown in the Fig(4.23). In the second case we take 200 coupled theta neurons in which 150 neurons are excitatory and 50 are inhibitory neurons. Each neuron receives the same input  $\beta_i = 0.1$  and there is all to all random coupling with the coupling strength varying between 0.05 and 0.1 and with different initial conditions. This simulation is shown in the Fig(4.24). The red colour neurons are the excitatory ones and the green coloured ones are inhibitory. On introducing Gaussian white noise of strength  $\sigma = 5.0$  into the system we observe synchronous phenomena emerging between the excitatory and inhibitory neurons. The interesting thing to note here is that most of the inhibitory neurons are firing in sync with other inhibitory neurons and also most of them are synchronized with excitatory neurons. This simulation is quite near to real ensembles of neurons for two reasons: first because the couplings have random strengths

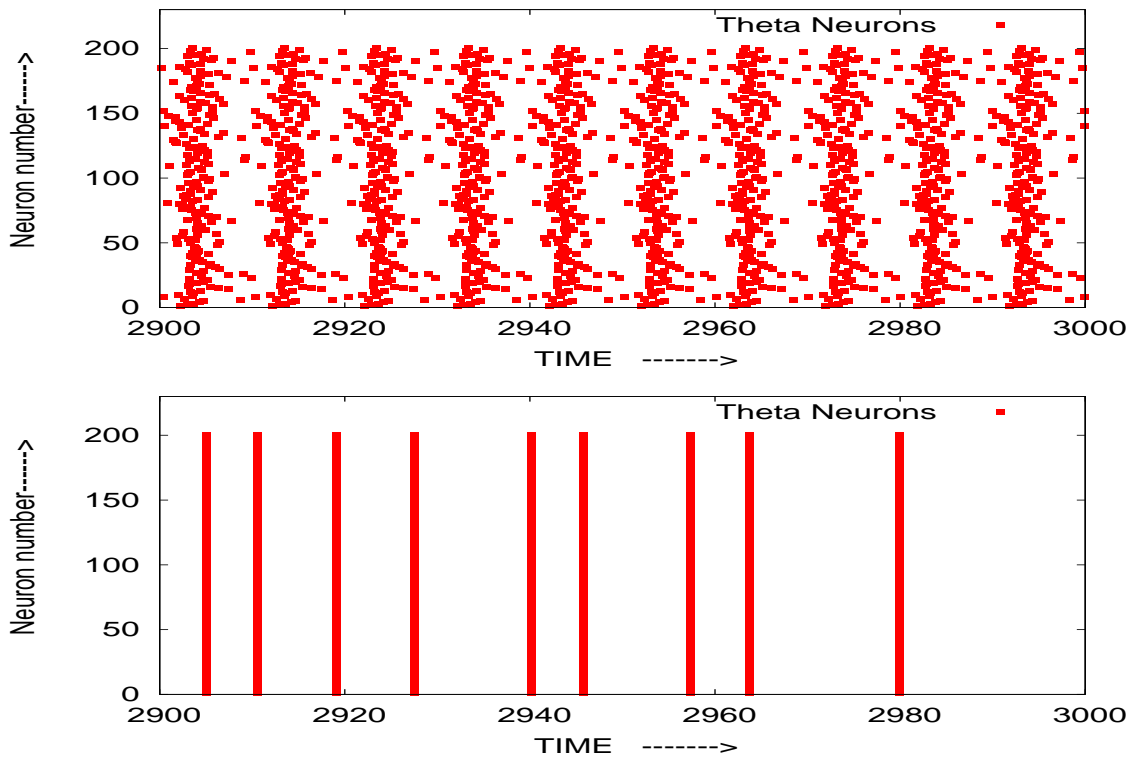


Figure 4.23: 200 uncoupled theta neurons, Above: in absence of noise, Below: in presence of noise  $\sigma = 0.25$

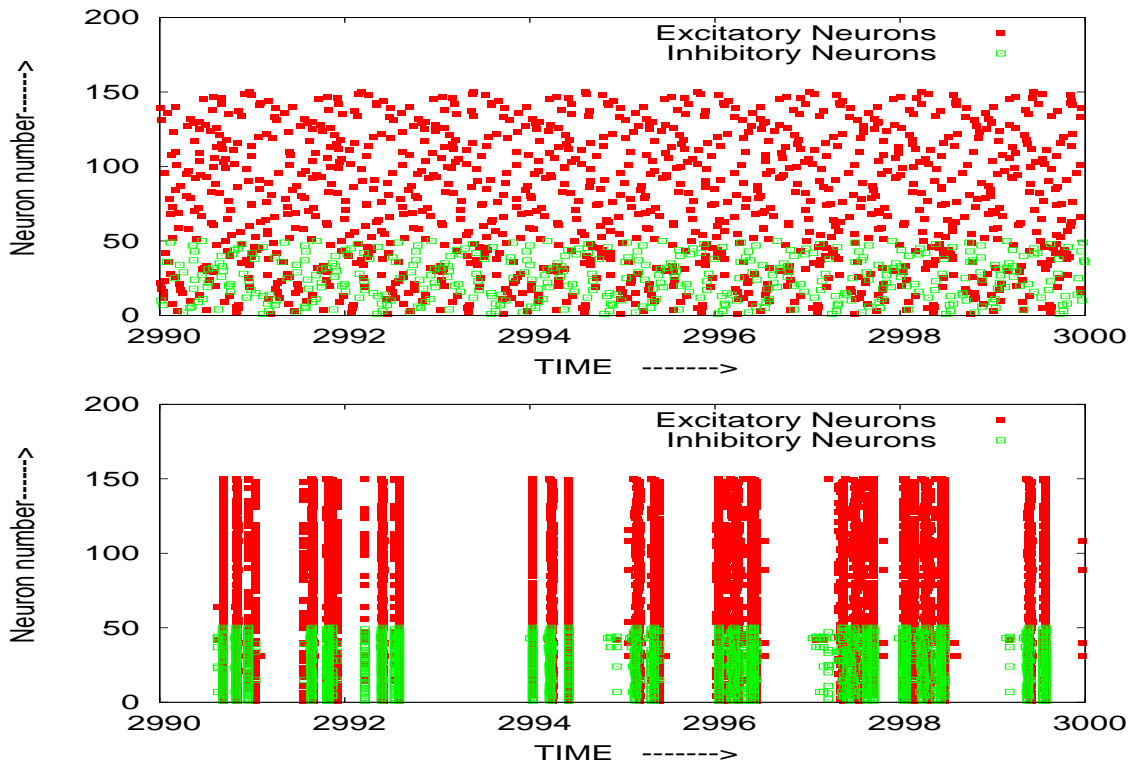


Figure 4.24: 200 uncoupled theta neurons, Above: in absence of noise, Below: in presence of noise  $\sigma = 5.0$

and second because these are all type I neurons and mammalian neurons exhibit type I excitability. This kind of noise induced complete synchronization with random coupling strengths has never been shown before for type I neurons.

## 4.9 Further studies and Conclusion

### 4.9.1 Further Studies

#### Noise induced order in IE system

We have shown that nearly complete synchronization can be possible even for IE systems in the presence of noise – an important result which is previously unknown in the literature. We have also observed noise induced co-operative phenomena such as noise induced phase synchronization discussed in Section(4.7). Here we display some more curves which show some kind of noise induced order in IE case for just two neurons. The values of parameters were the same as used earlier. In Fig(4.25) we see a zig-zag trajectory, which we get by joining the points in the bifurcation diagram we have shown in the last chapter for the IE case. But in the next figure(4.26) where we introduced noise of strength  $\sigma = 1.0$  we observe a smooth trajectory. This phenomenon is of course counter-intuitive as noise is always equated with disorder but here we observe order emerging on introducing noise. It is these kind of phenomena which need to be looked into further for correlating them with the dynamics of real neurons.

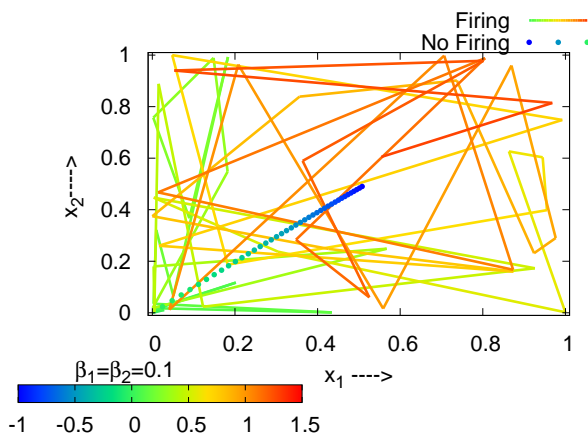


Figure 4.25: In absence of noise

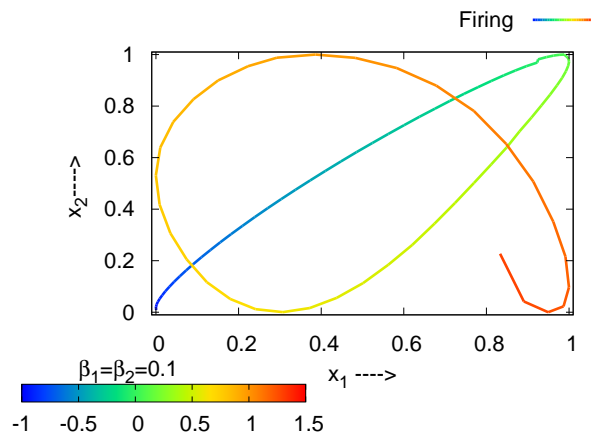


Figure 4.26: In presence of noise ( $\sigma = 1.0$ )

## Critical slowing down

In section(4.5) we have shown complete synchronization in a system of two coupled EE theta neurons firing at different initial conditions. There we observed noise induced transition to synchronization. Noise induced synchronization is mathematically not a well understood phenomenon. Since the phenomenon has many applications in many disciplines, therefore it is important to look into the origin of this kind of transition. Synchronization is thought to be a dynamics of the system rather than a state[2]. We explored [5],[6],[7] the possibility of the phenomenon of synchronization being effected through some kind of a bifurcation induced by noise. This kind of study can give us insights into the basic origin of noise induced synchronization. In Fig(4.27) for the same parameter values as used in Section (4.5) for showing CS in EE case we plot the  $\Delta t$  vs time where  $\Delta t$  is the difference in time taken by one iteration between the noiseless case and the case in which noise induces complete synchronization. The colour code represents the difference between outputs i.e  $x_1 - x_2$  (see Fig(4.27)). As the transition to synchronization starts the colour changes to black and there we see a broad spike which seems to be representative of critical slowing down of the system at that point. But to establish this fact beyond all doubt further studies needed to be done for this system.

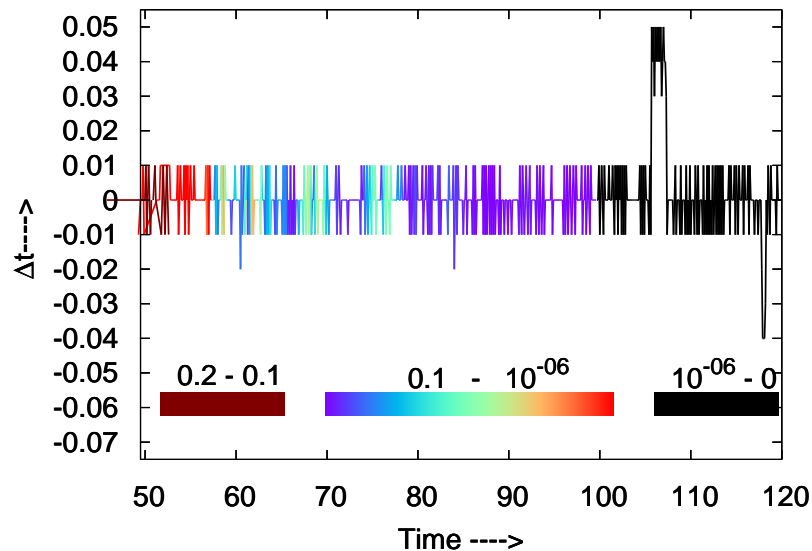


Figure 4.27: Synchronization as phase transition

## 4.10 Conclusion

The generic normal form equations which model type I neural excitability support a saddle node bifurcation on an invariant circle. The theta neuron model is described by such generic equations. So, it is mathematically plausible to reduce any physical or biological model having type I excitability to the theta neuron model by appropriate transformation of the variables involved. The major advantage of working with the theta neuron model is that it is governed by single variable allows for automatic phase resetting, and enables comparatively manageable simulations especially of bigger ensembles of neurons.

One of the possible mechanisms for synchronization in neurons could be due the presence of noise. Although even in a deterministic system, an appropriate coupling itself can lead to synchronization in oscillators, a more realistic situation should necessarily include fluctuations, since noise is part and parcel of all physical and biological systems including neurons and must be taken into account. We have studied in this dissertation noise induced synchronization in theta neurons. We have found that identical neurons firing at different initial conditions undergo complete synchronization on introducing Gaussian white noise into the system. Also we have observed that noise can induce variability in firing patterns. Naturally occurring systems are usually non identical and we have shown that noise is able to induce order and establish a co-operative phenomena in those cases also, especially phase synchronization of IE systems which has importance in the way neurons encode information.

We also carried out a 200 neuron simulation with random all to all couplings with 150 excitatory and 50 inhibitory neurons, we noticed in these simulation emergence of synchrony even between non-identical oscillators. An unexpected result we find is that it is possible in the presence of noise to induce nearly complete synchronization in an ensemble of IE neurons – a system of non-identical oscillators.

Nearly all the numerous results presented in this dissertation are new and have been shown for the first time (refs.[5],[6],[7]). It is hoped that our work would significantly further the understanding of physical and biological systems having the generic behaviour discussed herein.

# Appendix A

## Lyapunov Exponents

Before defining Lyapunov exponents we detail the notations and concepts we will be using in this section. The first among these is a variational equation.

### Variational Equation

Let us consider an  $n$ th order autonomous system

$$\dot{\mathbf{x}} = \mathbf{f}(\mathbf{x}) \tag{A.1}$$

where  $\mathbf{x}$  is an  $n$  dimensional vector. Let its solution at time  $t$  starting with initial condition  $\mathbf{x}(0) = \mathbf{x}_0$  be represented by  $\mathbf{F}_t(\mathbf{x}_0)$ . Then Eq(A.1) can be written as

$$\frac{d}{dt}\mathbf{F}_t(\mathbf{x}_0) = \mathbf{f}(\mathbf{F}_t(\mathbf{x}_0)) \tag{A.2}$$

Differentiating the above equation with respect to  $\mathbf{x}_0$  and using the chain rule we obtain

$$\frac{d}{dt}\mathbf{D}_{\mathbf{x}_0}\mathbf{F}_t(\mathbf{x}_0) = \mathbf{D}_{\mathbf{x}}\mathbf{f}(\mathbf{F}_t(\mathbf{x}_0))\mathbf{D}_{\mathbf{x}_0}\mathbf{F}_t(\mathbf{x}_0) \tag{A.3}$$

This equation is known as the variational equation of the differential equation. We simplify the notation by denoting

$$\mathbf{X}_t(\mathbf{x}_0) = \mathbf{D}_{\mathbf{x}_0}\mathbf{F}_t(\mathbf{x}_0) \tag{A.4}$$

So our variational equation in terms of this matrix will be

$$\dot{\mathbf{X}}_t(\mathbf{x}_0) = \mathbf{D}_{\mathbf{x}_0}\mathbf{F}_t(\mathbf{x}_0)\mathbf{X}_t(\mathbf{x}_0) \tag{A.5}$$

The above equation is the variational equation which we will be using in our algorithm for finding the Lyapunov exponent. It is basically a linearization of the vector field  $\mathbf{f}(\mathbf{x})$

along the solution. Also since  $\mathbf{F}_0(\mathbf{x}_0) = \mathbf{x}_0$ , hence  $\mathbf{D}_{\mathbf{x}_0}\mathbf{F}_t(\mathbf{x}_0) = \mathbf{I}$  i.e  $\mathbf{X}_0(\mathbf{x}_0) = \mathbf{I}$ . The importance of variational equation is in the fact that we can find the time evolution of a perturbation  $\delta\mathbf{x}_0$  of  $\mathbf{x}_0$  by

$$\delta\mathbf{x} = \mathbf{X}_t(\mathbf{x}_0)\delta\mathbf{x}_0 \quad (\text{A.6})$$

where  $\mathbf{X}_t(\mathbf{x}_0)$  comes from the solution of the variational equation.

## Definition of Lyapunov exponent

Let  $k_1(t), k_2(t), k_3(t), \dots, k_n(t)$  be the eigen values of the matrix  $\mathbf{X}_t(\mathbf{x}_0)$  where  $x_0$  is any initial condition picked from  $\mathbb{R}^n$ . Then the Lyapunov exponent is defined as

$$\lambda_i = \lim_{t \rightarrow \infty} \frac{1}{t} \ln |k_i(t)| \quad (\text{A.7})$$

A more practically useful definition for calculating Lyapunov exponents numerically could be given as follows: Two nearby initial conditions  $\mathbf{x}_0$  and  $\mathbf{x}'_0 = \mathbf{x}_0 + \delta\mathbf{x}_0$  evolve after some time  $t$  to  $\mathbf{x}$  and  $\mathbf{x} + \delta\mathbf{x}$ . The time evolution of a perturbation  $\delta\mathbf{x}$  of  $\mathbf{x}$  can be found by variational equation. The Lyapunov exponent can also be defined as the mean rate of divergence of two close trajectories. Thus we can write

$$\lambda(\mathbf{x}_0, \delta\mathbf{x}) = \lim_{t \rightarrow \infty} \frac{1}{t} \ln \frac{\|\delta\mathbf{x}\|}{\|\delta\mathbf{x}_0\|} \quad (\text{A.8})$$

where  $\|\cdot\|$  represents the Euclidean norm.

## Numerical calculation of Lyapunov exponent

A direct approach to calculate Lyapunov exponents from definition Eq(A.8) would involve finding out  $\mathbf{X}_t(\mathbf{x}_0)$  by solving the variational equation and then determining its eigen values using QR decomposition. But it is not workable in many cases in practice and we present a more sophisticated technique to find the Lyapunov exponent numerically. To calculate Lyapunov exponent of  $n$ th order continuous system Eq(A.1), we first integrate it to obtain a reference trajectory. Then simultaneously the variational equation Eq(A.5) is also solved starting with initial conditions defining an arbitrarily oriented frame of linearly independent n-orthonormal vectors  $(\delta\mathbf{x}_1, \delta\mathbf{x}_2, \delta\mathbf{x}_3, \dots, \delta\mathbf{x}_n)$  in  $\mathbb{R}^n$ . Usually there is a tendency of these orthonormal vectors when evolving in time: they line up in the direction

of most rapid growth. To overcome this we need to orthonormalise these vectors at regular intervals of time. For this purpose we use **Gram-Schmidt Orthonormalization** procedure which gives us a new set of vectors ( $\mathbf{u}_1, \mathbf{u}_2, \mathbf{u}_3, \dots, \mathbf{u}_n$ ) where

$$\begin{aligned}\mathbf{v}_1 &= \delta \mathbf{x}_1 \\ \mathbf{u}_1 &= \frac{\delta \mathbf{v}_1}{\|\mathbf{v}_1\|} \\ \mathbf{v}_i &= \delta \mathbf{x}_i - \sum_{j=1}^{i-1} \langle \delta \mathbf{x}_i, \mathbf{u}_j \rangle \mathbf{u}_j \\ \mathbf{u}_i &= \frac{\delta \mathbf{v}_i}{\|\mathbf{v}_i\|}\end{aligned}\tag{A.9}$$

where  $\langle \cdot \rangle$  denotes the inner product. The Gram-Schmidt Orthonormalization procedure is applied after a time interval  $\Delta t$  and the procedure as a whole is repeated  $N$  number of times the Lyapunov exponents are then given as

$$\lambda_i = \frac{1}{N\Delta t} \sum_{k=1}^N \ln \|v_i^{(k)}\|\tag{A.10}$$

## Algorithm for calculating Lyapunov exponent

Below we give an algorithm to calculate the Lyapunov exponent

**Step 1:-** Set the initial conditions

$\mathbf{u} = u[ ] = \mathbf{I}$  and  $\mathbf{x} = \mathbf{x}_0$

**Step 2:-** Set  $sum[ ] = 0$  and a counter  $i = 1$

**Step 3:-** Solve the Eq(A.1) with time step  $\Delta t$  to obtain  $\mathbf{F}_{\Delta t}(\mathbf{x}_0)$  and simultaneously solve the variational equation with the same time step  $\Delta t$ . Solution of variational equation will give us  $\mathbf{X}_{\Delta t}(\mathbf{x}_0)$ . Use it to solve  $\delta \mathbf{x} = \mathbf{X}_{\Delta t}(\mathbf{x}_0)\mathbf{u}$

**Step 4:-** Perform the Gram-Schmidt Orthonormalization on  $\delta \mathbf{x} = \delta \mathbf{x}[ ] [i]$  as discussed above and obtain  $\mathbf{v} = v[ ] [i]$

**Step 5** Calculate  $sum[i] = sum[i] + \ln \|v[ ] [i]\|$  then  $\lambda[i] = sum[i]/N\Delta t$

**Step 6** Increment  $i$  i.e  $i = i + 1$ . If  $i > i_{max}$  then Lyapunov exponents have not converged. Go to Step 8

**Step 7** Go to step 2 if required accuracy hasn't been achieved.

**Step 8** End

Most of the analysis and algorithm presented above is adapted from the book by Chua and Parker[41], a useful discussion is also given in [42] and [12]. A primitive form of this

algorithm in the form of a Fortran code is given in [43]. Other important references for the numerical calculation of Lyapunov exponent are [44] and [45].

Table A.1: Values of Lyapunov exponents for different attractors/motion

<b>Steady State</b>	<b>Flow</b>	<b>Lyapunov Exponents</b>
Equilibrium point	point	$0 > \lambda_1 \geq \dots \geq \lambda_n$
Periodic	Circle	$\lambda_1 = 0$ and $0 > \lambda_2 \geq \dots \geq \lambda_n$
Two Periodic(Quasi-Periodic)	torus	$\lambda_1 = \lambda_2 = 0$ and $0 > \lambda_3 \geq \dots \geq \lambda_n$
K-Periodic(Quasi-Periodic)	K-torus	$\lambda_1 = \lambda_2 = \lambda_3 = 0$ and $0 > \lambda_4 \geq \dots \geq \lambda_n$
Chaotic	Cantor-like	$\lambda_1 > 0$ and $\sum \lambda_i < 0$

# Appendix B

## Hilbert Transform

It is possible to obtain instantaneous attributes of a signal by using the technique of Hilbert Transform. Below we present a brief review of the basic concepts involved. Basic references for this is [46]. Also a useful note is also given in the appendix of ref.[2].

### Instantaneous Phase and Frequency

We define instantaneous phase and frequency using the definition given by van der Pol. Consider a simple harmonic motion by the expression

$$s(t) = A \cos(2\pi ft + \theta) \quad (\text{B.1})$$

Where  $A$  is the amplitude,  $f$  is the frequency and  $\theta$  is the phase constant. Then the instantaneous phase is defined as

$$\phi(t) = 2\pi ft + \theta(t) \quad (\text{B.2})$$

and the instantaneous frequency by

$$f_i(t) = \frac{1}{2\pi} \frac{d\phi(t)}{dt} \quad (\text{B.3})$$

### Analytical signal and Hilbert Transform

D.Gabor(1946) proposed a method of generating a complex signal from a real one. One can construct an analytical signal  $z(t)$  from a given signal  $s(t)$ . It is defined as

$$z(t) = s(t) + jH[s(t)] = A(t)e^{j\phi(t)} \quad (\text{B.4})$$

Where  $H[s(t)]$  represents the Hilbert Transform (HT) of  $s(t)$  and is given by

$$H[s(t)] = \pi^{-1} P.V \int_{-\infty}^{\infty} \frac{s(\tau)}{t - \tau} d\tau \quad (\text{B.5})$$

Where  $P.V$  denotes that the integral is taken in the sense of Cauchy principal value. Numerically, in time domain HT can be done via convolution of the time series data with precomputed characteristic of the filter(Hilbert Transform). The software package MATLAB provides a function **hilbert()** which can perform HT. Then instantaneous attributes can be calculated as follows.

Instantaneous phase :-

$$\phi(t) = \tan^{-1} \left( \frac{H[s(t)]}{s(t)} \right) \quad (\text{B.6})$$

Instantaneous amplitude :-

$$A(t) = \sqrt{s^2(t) + H[s(t)]^2} \quad (\text{B.7})$$

Instantaneous Frequency :-

$$f_i(t) = \frac{d\phi}{dt} = \frac{\phi(t_2) - \phi(t_1)}{t_2 - t_1} \quad (\text{B.8})$$

# Appendix C

## Stochastic RK-4

The major reference for this appendix are R uemelin[47],Hansen and Penland[48] and the book by Kloeden and Platen[49].The reference for deterministic RK-4 (Runge-Kuta 4th order) can be found in [50].

### Stochastic Differential Equation (SDE)

A SDE has the following form

$$d\mathbf{x} = \mathbf{F}(\mathbf{x}, t)dt + \mathbf{G}(\mathbf{x}, t) \circ d\mathbf{W} \quad (\text{C.1})$$

Where  $\mathbf{x}$  is stochastic variable,  $\mathbf{F}(\mathbf{x}, t)$  is the vector function of deterministic part and  $\mathbf{G}(\mathbf{x}, t)$  is the matrix containing the stochastic part.  $\mathbf{W}$  represents a Wiener process. The symbol  $\circ$  represents that integration is carried out in a stochastic sense using Stratonovich Calculus. Eq(C.1) can also be written as

$$\frac{d\mathbf{x}}{dt} = \mathbf{F} + \mathbf{G} \circ \frac{d\mathbf{W}}{dt} \quad (\text{C.2})$$

To solve the above equation numerically we need to discretize it. We know that  $dW_i$  has statistics of  $N(0, dt)$ , so if we write the discretized form of the Eq(C.2) as

$$\frac{d\mathbf{x}}{dt} = \mathbf{F} + \mathbf{G} \frac{\mathbf{z}}{\Delta} \quad (\text{C.3})$$

then  $\frac{\mathbf{z}}{\Delta}$  will be given by random number independently drawn from  $N(0, \frac{1}{\Delta})$ . That means the variance  $\sigma^2 \equiv \frac{1}{\Delta}$ , and therefore the standard deviation  $\sigma = \frac{1}{\sqrt{\Delta}}$ . Thus on normalizing  $N(0, 1)$  by  $\frac{1}{\sqrt{\Delta}}$  we can get the distribution similar to  $\frac{\mathbf{z}}{\Delta}$ . The stochastic RK-4 scheme is

as follows. Defining and updating the equation as

$$\mathbf{x}(t + \Delta) = \mathbf{x} + \sum_{j=0}^m p_j \mathbf{K}_j \Delta + \sum_{j=0}^m q_j \mathbf{M}_j \mathbf{z} \quad (\text{C.4})$$

where

$$\mathbf{K}_0 = \mathbf{F}(\mathbf{x}(t), t + \nu_0 \Delta) \quad (\text{C.5})$$

$$\mathbf{M}_0 = \mathbf{G}(\mathbf{x}(t), t + \nu_0 \Delta) \quad (\text{C.6})$$

$$\mathbf{x}^{(1)} = \mathbf{x}(t) + \beta_{1,0} \mathbf{K}_0 \Delta + \gamma_{1,0} \mathbf{M}_0 \mathbf{z} \quad (\text{C.7})$$

$$\mathbf{K}_1 = \mathbf{F}(\mathbf{x}^{(1)}(t), t + \nu_1 \Delta) \quad (\text{C.8})$$

$$\mathbf{M}_1 = \mathbf{G}(\mathbf{x}^{(1)}(t), t + \nu_1 \Delta) \quad (\text{C.9})$$

$$\mathbf{x}^{(2)} = \mathbf{x}(t) + (\beta_{2,0} \mathbf{K}_0 + \beta_{2,1} \mathbf{K}_1) \Delta + (\gamma_{2,0} \mathbf{M}_0 + \gamma_{2,1} \mathbf{M}_1) \mathbf{z} \quad (\text{C.10})$$

.

.

.

$$\mathbf{x}^{(m)} = \mathbf{x}(t) + \sum_{k=0}^{m-1} \beta_{m,k} \mathbf{K}_k \Delta + \sum_{k=0}^{m-1} \gamma_{m,k} \mathbf{M}_k \mathbf{z} \quad (\text{C.11})$$

$$\mathbf{K}_m = \mathbf{F}(\mathbf{x}^{(m)}(t), t + \nu_0 \Delta) \quad (\text{C.12})$$

$$\mathbf{M}_m = \mathbf{G}(\mathbf{x}^{(m)}(t), t + \nu_0 \Delta) \quad (\text{C.13})$$

The conditions on above coefficients are as for Stratonovich calculus and are as follows  $\sum_{j=0}^m p_j = 1, \sum_{j=0}^m q_j = 1$  and  $\lambda = \sum_{j=1}^n q_j \sum_{k=0}^{j-1} \gamma_{j,k} = 1/2$ . The values of other parameters are:  $p_0 = p_3 = q_0 = q_3 = 1/6, p_1 = p_2 = q_1 = q_2 = 1/3, m = 3, \nu_0 = 0, \nu_1 = \nu_2 = 1/2, \nu_3 = 1, \beta_{1,0} = \beta_{2,1} = \gamma_{1,0} = \gamma_{2,1} = 1/2, \beta_{2,0} = \beta_{3,0} = \beta_{3,1} = \gamma_{2,0} = \gamma_{3,0} = \gamma_{3,1} = 0, \beta_{3,2} = \gamma_{3,2} = 1$ . It is very much clear from the step one that this algorithm proceeds by drawing  $\mathbf{z}$  from  $N(0, \Delta)$ . The advantage of working with this method is that it is many time less expensive than traditional methods like Euler's method. It is compact, so easy to code. We have chosen this method because of its speed as we were required to solve 400 coupled equations for the 200 neuron simulations. Gaussian white noise is generated using **Box-Muller method**[51].

# Bibliography

- [1] S.Strogatz, *Sync: The Emerging Science of Spontaneous Order* (Hyperion, New York, 2003).
- [2] A. Pikovsky, M. Rosenblum, and J. Kurths, *Synchronization: A Universal Concept in Nonlinear Sciences* (Cambridge University Press, Cambridge, 2001).
- [3] L. Glass, *Nature* **410**, 277 (2001).
- [4] V. Anishchenko *et al.*, *Nonlinear Dynamics of Chaotic and Stochastic Systems:Tutorial and Modern Developments* (Springer, Berlin, 2002).
- [5] Nishant Malik, J.Balakrishnan, and B.Ashok,*Noise-induced synchronous activity in coupled theta neuron* Proceedings of the fourth National Conference on Nonlinear Systems and Dynamics, Jan 3-5, 2008, Physics Research Laboratory, Ahmedabad. Online version at: <http://www.cts.iitkgp.ernet.in/ncnsd/proceeding08/ccs.php>
- [6] Nishant Malik, J.Balakrishnan, and B.Ashok, *Noise-induced firing and synchronization in a system of coupled theta neurons*(2008)(Submitted)
- [7] Nishant Malik, J.Balakrishnan, and B.Ashok, *Synchronization in coupled Class I neurons: the role of noise*(2008)(Submitted)
- [8] G.B.Ermentrout, *Neural Comp.* **8**, 979 (1996).
- [9] E.M.Izhikevich, *Int.J.Bif. & Chaos* **10**, 1171 (2000).
- [10] P. Laurent, *Science* **45**, 44 (1917).
- [11] C.Zhou and J.Kurths, *Phys. Rev. Lett.* **88**, 230602 (2002).
- [12] K.T.Alligood, J.A.Yorke, and T.D.Sauer, *CHAOS: An Introduction to Dynamical Systems* (Springer, New York, 1996).

- [13] L.M.Pecora and T.Carroll, Phys. Rev. Lett. **64**, 821 (1990).
- [14] H.D.I.Abarbanel, *Analysis of Observed Chaotic Data* (Springer, New York, 1996).
- [15] V.Petrov, Q.Quyang, and H.L.Swinney, Nature **388**, 655 (1997).
- [16] T. J.Walker, Science **166**, 891 (1969).
- [17] J.Buck and E. Buck, Science **159**, 1319 (1968).
- [18] A. H. B. Blasius and L. Stone, Nature **399**, 354 (1999).
- [19] W.Singer, Neuron **24**, 49 (1999).
- [20] E.M.Izhikevich, *Dynamical Systems in Neuroscience:The Geometry of Excitability and Bursting* (MIT Press, Cambridge,Massachusetts, 2006).
- [21] A.Scott, *Neuroscience:a mathematical primer* (Springer, New York, 2002).
- [22] P.Dayan and L.F.Abbott, *Theoretical Neuroscience* (MIT Press, Cambridge,Massachusetts, 2001).
- [23] E. Kandel, J.H.Schwartz, and T.M.Jessell, *Principles of neural science* (McGraw-Hill, New York, 2000).
- [24] A.L.Hodgkin and A.F.Huxley, J.of Physiol.(London) **117**, 500 (1952).
- [25] W. Gerstner and W. M. Kistler, *Spiking Neuron Models. Single Neurons, Populations, Plasticity* (Cambridge University Press, Cambridge, 2002).
- [26] C.Morris and H.Lecar, Biophys.J. **35**, 193 (1981).
- [27] A.L.Hodgkin, J.of Physiol.(London) **107**, 165 (1948).
- [28] J.Rinzel and G.B.Ermentrout, in *Methods in Neuronal Modeling*, edited by C.Koch and I.Segev (MIT Press, Cambridge,Massachusetts, 1998), pp. 135–169.
- [29] G.B.Ermentrout and N.Kopell, SIAM J.Appl.Math **46**, 233 (1986).
- [30] S.H.Strogatz, *Nonlinear Dynamics and Chaos with applications to Physics,Biology,Chemistry and Engineering* (Perseus Books, Massachusetts, 1994).

- [31] C.Börger and N.Kopell, *Neural Comp.* **15**, 509 (2003).
- [32] B.S.Gutkin and G.B.Ermentrout, *Neural Comp.* **10**, 1047 (1998).
- [33] W.Lim and S.-Y. Kim, *J. Korean Phys. Society* **50**, 219 (2007).
- [34] M.Wechselberger, *Canards* (Scholarpedia **2**(4):1356, <http://www.scholarpedia.org/article/Canards>, 2007).
- [35] C. V. Vreeswijk, L. Abbott, and G.B.Ermentrout, *J. Comp. Neuroscience* **1**, 313 (1994).
- [36] C.Koch, *Biophysics of computation:Information processing in single neurons* (Oxford University Press, New York, 1999).
- [37] A.Longtin, *J. Stat. Phy* **70**, 309 (1993).
- [38] A.Longtin, *Phys. Rev. E* **55**, 868 (1997).
- [39] B.Gutkin, T.Hely, and J.Jost, *Neurocomputing* **58**, 753 (2004).
- [40] R.L.Stratonovich, *Topics in the Theory of Random Noise* (Gordon and Breach, New York, 1963).
- [41] T. Parker and L.O.Chua, *Practical Numerical Algorithms for Chaotic Systems* (Springer, New York, 1990).
- [42] M.Lakshmanan and S.Rajasekar, *Nonlinear Dynamics: Integrability,Chaos and Patterns* (Springer, New Delhi, 2003).
- [43] A.Wolf, J.B.Swift, H. Swinney, and J. Vastano, *Physica D* **16**, 285 (1985).
- [44] J.P.Eckmann and D.Ruelle, *Rev. Mod. Phys.* **57**, 617 (1985).
- [45] J. Gao and Z. Zheng, *Phys. Rev. E* **49**, 3807 (1994).
- [46] B.Boashash, *Proc. IEEE* **80**, 520 (1992).
- [47] W.Rümelin, *SIAM J.Numer.Anal.* **19**, 604 (1982).
- [48] J. Hansen and C.Penland, *Monthly Weather Rev.* **134**, 3006 (2006).

- [49] P. Kloeden and E. Platen, *Numerical solution of Stochastic Differential Equations* (Springer-Verlag, Berlin, 1992).
- [50] W. H. Press, S. A. Teukolsky, W. T. Vetterling, and B. P. Flannery, *Numerical Recipes in C*, 2nd ed. (Cambridge University Press, Cambridge, 1992), Chap. 16, p. 707.
- [51] J. E. Gentle, *Random Number Generation and Monte Carlo Methods*, 2nd ed. (Springer, New York, 2003), Chap. 5, p. 165.